INVESTIGATION OF THE GOUGING ABRASION RESISTANCE OF MATERIALS IN THE MINING INDUSTRY

by

DONALD TOLFREE

B. Eng, McGill University, 2000

THIS THESIS IS SUBMITTED FOR THE PARTIAL FULFILMENT OF THE REQUIREMENTS FOR THE DEGREE OF

MASTER OF APPLIED SCIENCE

in

THE FACULTY OF GRADUATE STUDIES

DEPARTMENT OF MINE ENGINEERING

We accept this thesis as conforming to the required standard

The University of British Columbia

September, 2004

Library Authorization

Donald Tolfree
Name of Author *(please print)*

27-09-2004.
Date (dd/mm/yyyy)

Title of Thesis: Investigation of the Gouging Abrasion Resistance of materials in the Mining Industry

Degree: Master of Applied Science Year: 2004.

Department of Mine Engineering.
The University of British Columbia
Vancouver, BC Canada

Abstract

With increased budget constraints, innovative cost reduction methods are required to increase the profitability of today's mines. Abrasive wear reduction is a novel way to reduce costs and increase productivity. Specifically, gouging abrasion is making an increased contribution to abrasive wear losses in the oil sands industry. To assess material property requirements for mitigating this wear mechanism, jaw crusher gouging abrasion tests using a modified ASTM G81 procedure, have been carried out on a range of wear materials of interest for oil sands mining service. The method involves a comparison of the wear losses that occur for reference and selected test plates when a controlled amount of standard feed rock is comminuted in a laboratory jaw crusher. Among the classes of material evaluated have been Q&T plate steels, austenitic manganese steel, chromium and chromium molybdenum white irons as plain castings and in laminated forms and also chromium carbide and tungsten carbide overlaid wear plates. In addition, the initial stages of relationships are presented relating wear rates/factor, determined from the laboratory gouging abrasion test, to the quartz content of the abrasive material. Of all the materials tested, the laminated CrMo white consistently had the lowest wear factor (best gouging abrasion resistance). From the data produced by this work, the wear factor has a linear relationship with quartz, while the wear rate has a non-linear relationship.

Table of Contents

List of Figures

List of Tables

Acknowledgments

The completion of this work would not have been possible without the help of a variety of people;

Frank Schmidtiger from University of British Columbia and Andrew Mattie from the National Research Council were instrumental in helping setup the jaw crusher at the University of British Columbia.

Dilip Kumar and Cathy Ng demonstrated patience and understanding while helping me with some of the technical equipment used to analyze the post test wear plates in the laboratory at the National Research Council.

Specific thanks go to Dr. Mario Morin and Dr. Robert Hall for their guidance in writing and formatting the thesis.

Finally thanks to Dr. Rees Llewellyn for his overall support. It was his expertise that helped explain some of the more technical material sciences concepts and to explain some of the ambiguity in mining wear research today.

1.0 Introduction

In today's mines, the mine engineer is typically concerned with such issues as ground control, production sequencing and equipment utilization to produce enough ore to pay the operating expenses, payback the capital cost and make a profit. With increased budget constraints, there is a desire to find innovative ways to increase production and/or reduce operating costs to make operations more profitable. The understanding of wear and improved wear protection practice are ways to reduce operating costs and increase production. Wear is an unavoidable part of mining, wherever metal comes in contact with rock, there is wear. Because of the complex and variable nature of wear, remedial measures to reduce it are not always the same; adding a lubricant is a simple way to decrease adhesive wear, but will not reduce abrasive wear. In addition, improved wear materials are an investment in reliability. For example, certain situations require an investment in more expensive, more wear-resistant materials (i.e. areas where unexpected shut downs or frequent down times reduces the production of the mine such as a primary crusher), while others do not require the extra investment (i.e. infrequently used machines or machines whose down time is not critical to production such as the lip on the blade of a dozer).

The study of wear falls under the domain of the tribologist. According to the Merriam Webster dictionary, tribology is "a study that deals with the design, friction, wear, and lubrication of interacting surfaces in relative motion (as in bearings or gears)". The word was originally coined in 1966 by Peter Jost in his paper on friction and lubrication. It incorporates the three different fields of friction, wear and lubrication.

Each belongs to its own unique field of research, friction belonging typically to the physics community; wear to the material science community; and lubrication to the chemistry and chemical engineering community (Encyclopedia Britannica, 2004). The wear of materials is normally defined as the "removal of a material from a solid surface through mechanical interaction" (Rabinowicz, 1995, pg 124).

According to U.S. researchers, wear accounted for up to 6% of the U.S. GNP in 1983, while only receiving 0.02% of the yearly research funds (Rabinowicz, 1995). Past researchers have stated that wear and wear rates are so "complicated and erratic that systematic research was bound to be a waste of time" (Rabinowicz, 1995, pg 126). In a strategy manual for dealing with tribology, published by the National Research Council of Canada, reference was made to the estimated loss due to friction and wear in Canadian industry. The study includes the agriculture, electric utilities, forestry, mining, pulp and paper, rail and road transportation and wood industries. It estimated that losses due to wear, in 1982 Canadian dollars, were in the neighborhood of $3.9 billion dollars (A Strategy for Tribology in Canada, 1993). A break down of cost per industry is shown in Table 1.

Table 1: Breakdown per industry of estimated losses due to wear (A Strategy for Tribology in Canada, 1993) Note: M$/a refers to millions of dollars per year.

Economic Sector	Friction		Wear		Total Losses (M$/a)
	Percentage of sector energy costs	M$/a	Percentage of sector maintenance costs	M$/a	
Pulp and Paper	8	105	54	382	487
Forestry	23	111	51	158	269
Mining					
-Refining	22	212	28	79	726
-Open Pit			72	259	
-Mills			82	327	
-Tar Sands			26	63	
Agriculture	17	321	82	940	1261
Transportation					
-Rail	51	284	23	466	750
-Trucks/Buses	18	126	42	861	987
Electric Utility	11	54	46	189	243
Wood Industries	14	14	65	189	203
Total		**1,227**		**3,913**	**5,140**

Table 2 is a further breakdown of the losses due to wear and friction in the mining industry according to the wear mechanism. According to the study, abrasion is the most costly wear mechanism in mills costing approximately 239 millions dollars a year.

Table 2: Breakdown of estimated losses due to wear in the mining industry (A Strategy for Tribology in Canada, 1993). Note: M$/a refers to millions of dollars per year.

	Wear Mechanisms (M$/a)						
Operation	Abrasion	Adhesion	Erosion	Fretting	Fatigue	Chemical	**Total Losses due to Wear M$/a**
Open Pit	230	10		1	16	1	**258**
Milling	239	1	72		4	11	**317**
Refining	44	3	24		3	4	**78**
Tar Sands	38	1	21		2	1	**63**
Total	**551**	**15**	**117**	**1**	**25**	**17**	**726**

This report was written in 1983, before major growth in the oil sands industry where abrasion/erosion is a very severe problem. They have recently switched to hydraulic

transportation requiring smaller particle sizes. The crushing required to reduce the particle size has increased gouging abrasion wear (Llewellyn, 2004c).

1.1 Objectives

Wear is an important factor that influences the costs of mining operations. One of the predominant types of wear seen is gouging abrasion. Due to the implementation of hydraulic transportation, gouging abrasion is making an increased impact in the oil sands industry (Llewellyn, 2004c) Thus, this thesis will focus on using standard tests to gain an understanding of the gouging abrasion properties of various materials and abrasives applicable to the industry. To accomplish this, the following specific objectives will be targeted.

- An evaluation of the gouging abrasion resistance of fifteen different materials presently in use in the oil sands industry. Of the fifteen different materials tested, published gouge abrasion data and analysis results exists for ten of them. For the remaining there is limited to no published gouge abrasion properties. Therefore a subset of this objective is to establish and compare gouging abrasion data on these materials.
- An evaluation of the influence of rock properties on gouging abrasion resistance of materials. This evaluation can lead to a relationship between rock properties and wear rates/factors. In addition established relationships will be used to ensure quality of the test results.
- Through documentation of the test results and summarization of the current literature on wear this thesis will attempt to explain wear to the mine engineer; by giving them a brief background in wear and wearing

mechanisms, by reinforcing the importance of materials sciences in abrasion/erosion resistance and providing the initial stages of relationships that can relate wear to rock mass properties.

2.0 Literature Review

2.1 Fundamentals of Wear

Wear can be organized according to different properties; the stress imposed on the materials, the material removal method or the number of bodies involved in the wearing process, to name a few. Together, the different classes can be confusing. This section will explain the main wearing mechanisms and categories. The goal is to outline a very general background in wear so that the influences wear has on the mining industry can be better understood. The main wear mechanisms affecting the mining industry will be presented in section 2.2.

2.1.1. Wear Mechanisms

Wear is a very complex subject. It is easy to measure but difficult to predict (Rabinowicz, 1995). There have been many attempts to establish a universal naming convention to characterize wear mechanisms, without success. A search of metal suppliers on the Internet produced different "main" wear mechanisms. According to Alloy Steel International there are five main types of wear; adhesion, abrasion, corrosion, high temperature and impact (Alloysteel, 2004). It is not uncommon to see wear described as cavitational, erosional or fretting (The British Gear Association, 2004); (A Strategy for Tribology in Canada, 1993). According to Rabinowicz in his book Friction and Wear of Materials, DeGee came up with a glossary of wear terms in 1969. According to the glossary, there are four main wear mechanisms; adhesion, abrasion,

corrosion and surface fatigue. The main reason for the different terminology is the highly variable nature of wear; it affects everything from clothes, to hydraulic hoses, to engines components and hip replacements. In addition, each situation usually has its own dominate wear mechanism and each part has its own tolerance for wear (Rabinowicz, 1995). For mining applications, a crusher can lose many centimeters worth of surface material before it is no longer able to perform its job. Whereas the pistons in a car engine can only lose approximately 0.5 cm before the performance is severely compromised. DeGee's 1969 glossary of terms will be taken as the main mechanisms of wear and they will follow Rabinowicz's 1995 definitions:

- Adhesive Wear
- Corrosive Wear
- Abrasive Wear
- Surface Fatigue
- Minor Types

Adhesive Wear

Pure adhesion is the most fundamental type of wear (Burwell, 1957); (Rabinowicz 1995). It is a result of the interaction of two materials with similar hardness and surface smoothness. There are no abrasive or corrosive particles present and there is no lubrication to protect the surfaces. Burwell describes the mechanical action of adhesive wear in terms of apparent and actual contact area. Under extreme magnification, the actual contact area is much smaller than the apparent contact area. The force holding the two materials together is transmitted through the actual contact area and results in extremely high stresses. The high stress allows the materials to be pressure-welded at the contract surface (Burwell, 1957); (Rabinowicz, 1995). Figure 1 schematically shows how

Burwell describes adhesion; where A_o is the apparent contact area of two smooth surfaces. The wave crests are the actual contact area.

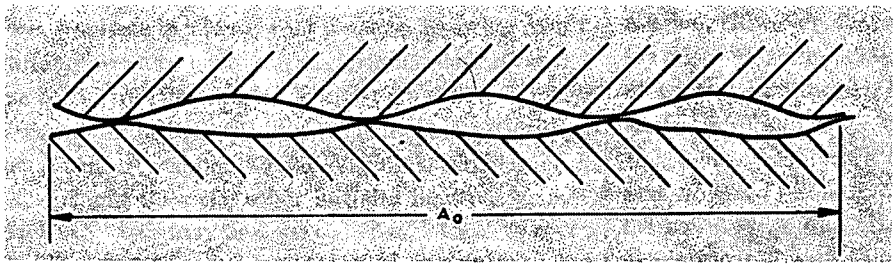

Figure 1: Burwell's demonstration of the difference between actual contact area and apparent contact area (A_o) (Burwell, 1957).

Corrosive Wear

Corrosive wear involves two actions. The first is the alteration of the surface chemistry of a material, typically making it weaker and easier to remove. The second is the sliding of one surface against another and the removal of the weakened skin. The removal of the skin offers a new clean surface to the corroding environment and the process continues (Rabinowicz, 1995). Figure 2 shows a micrograph of a corroded surface during the second step of corrosive wear. The surface has already been chemically altered and is in the process of flaking off. The micrograph also shows that corrosive wear extends only to a small depth below the surface.

It is generally accepted that wear is a mechanical attack, while corrosion is a chemical attack. Although corrosive wear has a minimal contribution to the overall cost of wear in the mining industry, from the author's experience it is influential in the quality of ground support in high sulphide ore bodies. As water trickles through the ore body, it mixes with the sulphides typically found in pyritic minerals. The solution becomes acidic and is capable of corroding installed ground support. Installed thread bars are placed

under a mechanical load; the corrosion weakens the thread bar, making it no longer able to hold the load and it fails. For this reason, in areas of high pyrite content remedial measures such as thicker gauge screen, galvanized split sets and fully grouted rebars are taken to protect and ensure the life of the installed support.

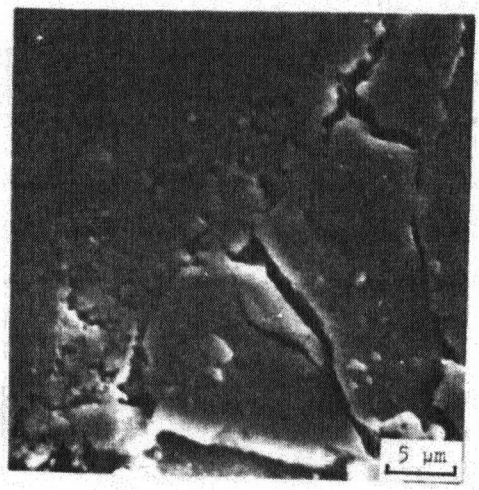

Figure 2: The second step in corrosive wear. A skin on the material has been chemically altered and is flaking off (Burwell, 1979).

Abrasive Wear

Abrasive wear is considered the most damaging of the wear mechanisms (Burwell, 1957); (Rabinowicz, 1995). Abrasion is common when two materials with different hardness are in contact. Abrasive wear is the removal of a softer material by a harder material. This type of wear is often visible with the naked eye (Burwell, 1957), examples of it are shown in Figure 3. Typically material removal during abrasion comes in the form of micro-cracking, micro-fatigue, plowing, cutting and wedge failure (ASTM, 2004). Abrasive wear is the most common form of wear found in the mining industry and will be discussed in detail in section 2.2 (Llewellyn, 1996)

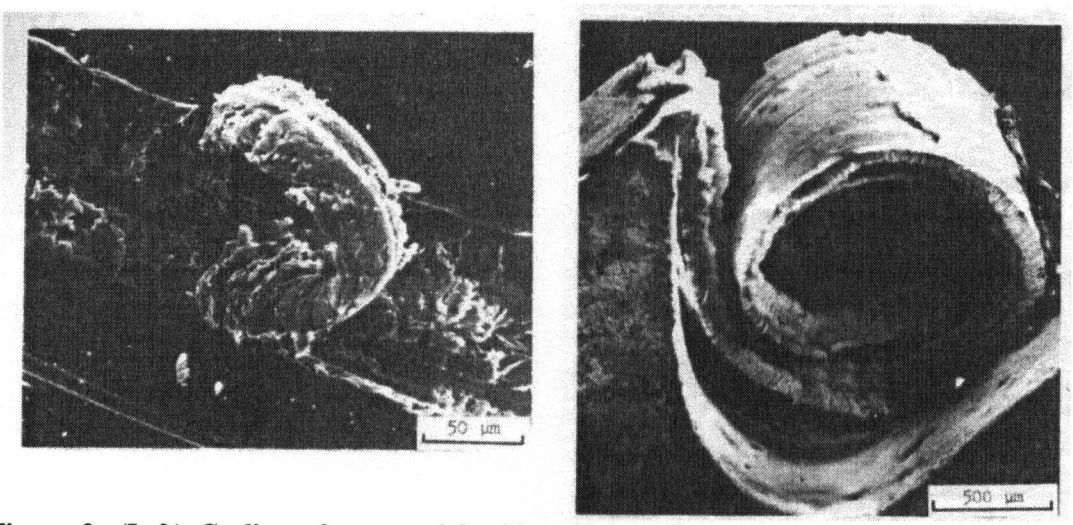

Figure 3: (Left) Curling of a material with evidence of some micro-cracking. (Right) Higher magnification of curling of a wear material (Burwell, 1979).

Surface Fatigue

The previous three forms of wear involve one material sliding, rolling or a combination thereof, over another material. They are mostly a one pass type of wear. Surface fatigue is a cyclical type of mechanical or thermal failure (SME Mining Handbook, 1992). A surface fatigue type of scar is normally larger and causes more damage than the wear scars caused by the other types of wear. Burwell describes surface fatigue through the use of the Hertz Equations for elastic deformation.

> "....The Hertz equation for elastic deformation of solid bodies shows the maximum shear stress does not occur immediately at the surface, rather at a small distance below the surface."(Burwell, 1979) Refer to Figure 4.

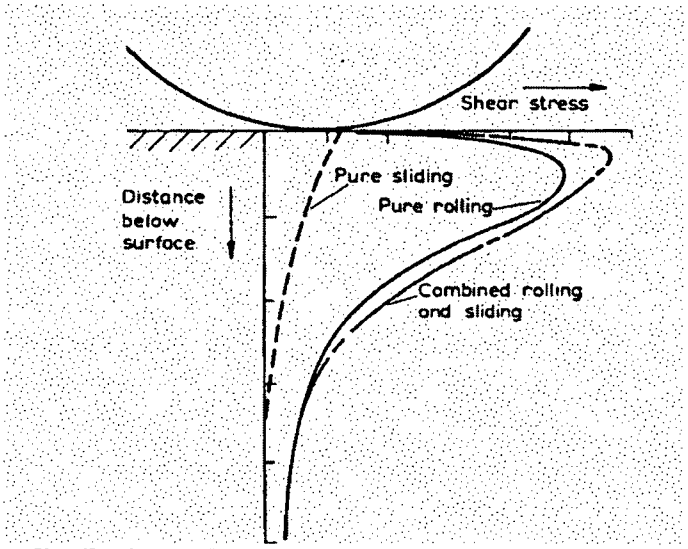

Figure 4: Shear stress distribution under repeated rolling, sliding or a combination causing surface fatigue wear (Burwell, 1979).

The shear stress in the figure never reaches the elastic limit. It is the repeated action of rolling or sliding over the surface that causes the fatigue failure. According to Figure 4, the shear stress reaches its maximum slightly below the surface. For "normal" ball bearings the depth is in the order of 0.25 mm (Rabinowicz, 1995). Once a fatigue crack develops slightly below the surface of a material, it will continue to propagate until failure. Eventually the material above the crack will flake out leaving the surface badly pitted. Figure 5 shows the results of the surface fatigue type of wear on a ball bearing. As can be seen in the micrograph, there are bulges on the left hand side of the failure. The bulges indicate which way the ball was rolling.

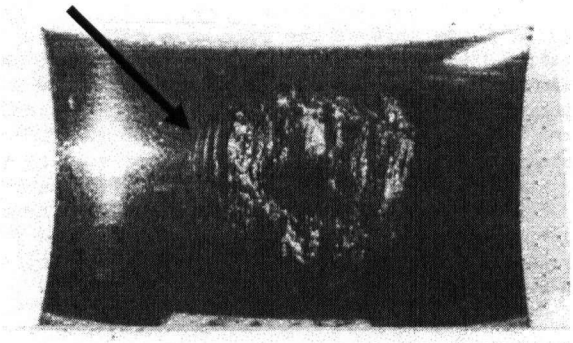

Figure 5: Surface fatigue type of wear on a ball bearing. Arrow pointing to bulges characteristic of surface fatigue failure (Burwell, 1979).

Minor Types

While the four main mechanisms, or combinations thereof, deal with most wear situations, there are other types of wear that are equally as common such as erosive, impact and cavitational wear (The British Gear Assocation, 2004). Table 3 shows a list of other possible wear mechanisms encountered and a grouping of a suggested hierarchy (Burwell, 1979). The list is by no means a compilation of every wear mechanism, but shows how difficult identifying the main wearing mechanisms for all wear can be. From the table on the right hand side, it is rare that one wearing mechanism is present by itself. Under the suggested corrosive category, Burwell has place abrasion; while abrasion is a main category in itself. The two wearing mechanisms sometimes work in conjunction with each other, increasing the amount and rate of attack and is the reason for the overlap (Burwell, 1979).

Examples of named wear mechanisms			
scratching	scavenging	cutting	gliding
grooving	scuffing	plucking	rolling
gouging	scraping	tearing	deformation
ploughing	galling	spalling	shear
chipping	rubbing	scaling	welding
snaring	sliding	crushing	melting
adhesion	impact	diffusion	
abrasion	percussion	corrosion	
corrosion	pitting	phase transformation	
erosion	chattering	surface fracture	
cavitation	fretting		
attrition	delamination		
	fatigue		

Suggested hierarchic arrangement	
abrasion	**erosive**
gouging	corrosion
cutting	abrasion
deformation	fatigue
adhesion	**corrosive**
adhesion	abrasion
deformation	impact
shearing	fatigue
	corrosion

Table 3: (Left) List of other wear mechanisms encountered and (right) a suggested grouping of wear terms under four principal wear mechanisms (Burwell, 1979).

2.1.2 Wear Categories

In order to classify the highly variable nature of wear for laboratory tests, different terminology has evolved to describe the different tribo-systems. There are two main classification systems, which are normally used along side each other, which causes some of the ambiguity seen in literature today (Gates, 1998). This section will explain the two classifications used to describe the different systems.

High Stress, Low Stress and Gouging Abrasion

This classification system uses the stresses imposed on the wear components to classify the tribo-system. Low stress, high stress and gouging abrasion are more commonly used when referring to abrasive wear. Low stress abrasion does not impart enough force to crush the abrasive. High stress abrasion imparts enough force on the abrasive to crush it. The contact stresses in gouging abrasion are the highest of the three

forms described. (Gates, 1998);(Trezona, 1999). This category is less confusing and more popular among researchers in wear in the mining industry.

Two-Body and Three-Body Abrasion

While the stress imposed on a particle is relatively straight forward, two-body or three-body abrasive wear is not. Historically, two-body abrasion involves the interaction of only two surfaces and three-body abrasion involves the interaction of three surfaces (Moore,1974); (Rabinowicz, 1961); (Gates, 1998). An example of two-body abrasion is machining a piece of steel. In this view, two-body abrasive wear causes about ten times more wear than three-body abrasive wear and is the equivalent of high stress abrasion (Rabinowicz, 1961);(Gates, 1998). By elimination, three-body wear must then be equivalent to low stress abrasion (Gates, 1998). The Pin-On-Drum test (explained separately in section 2.3.3) is considered to be a high stress, two-body abrasion test (The abrasion is caused by an Al_2O_3 abrasive cloth whose particles are not allowed to move). However, there are in reality three bodies present in the Pin-On-Drum test; the test material, the abrasive cloth and the backing plate applying the force to cloth (Gates, 1998). In addition, according to this train of thought, low stress is a characteristic of three-body abrasive wear. A rock sliding down a chute in a mine is an example of low stress abrasion however there are only two bodies present.

The recent trend in research is a modification to the definition of two or three body abrasion. If a particle is only allowed to slide during the wearing process then it is termed two-body abrasion (e.g the Pin-On-Drum test). Whereas if a particle is allowed a combination of sliding and rolling during the wearing process then it is referred to as

three-body abrasion (e.g. a shovel digging a pile of loose rock) (Stachowiak, 2004);(Gates, 1998). This view has the same problem as the first. A shovel digging a pile of loose rocks does not contain three bodies, there are only two bodies. In addition there are situations that are described as three body (sliding/rolling) abrasion such as the Dry Sand Rubber Wheel test (explained separately in section 2.3.3), when in fact the sand particles used in the test may actually be gripped by the rubber wheel and are not allowed to roll resulting in two-body (sliding) abrasion (Gates, 1998). It has been suggested in literature to drop the terms two-body and three-body (to reduce the confusion caused) and replace them with grooving or rolling abrasive wear (Trezona, 1999).

2.2 Wear in the Mining Industry

As mentioned previously, each industry has its own dominant wear mechanisms. Because mining is the removal, comminution and transportation of rocks and soils, its main wear mechanisms are abrasion and erosion. Corrosion also occasionally influences the abrasion and erosion rates. As a result there are sub categories of abrasion/corrosion and erosion/corrosion (Llewellyn, 1996). In addition to the wear mechanisms, there are many factors that influence most wear problems; the wear material, the abrasive that causes the wear and the design of the machine to name a few (Arnson, 1980). There is research in the drilling community, on the affect of different abrasives on the wearing mechanism and the amount of wear (Beste, 2004).

2.2.1 Wear Mechanisms

Abrasion

Abrasive wear can be separated into three categories according to the descriptions setout in section 2.1.2.

Low Stress Abrasion

Low stress abrasion occurs when there is not enough force applied to the abrasive to fracture it. It occurs mainly in chutes and screens where the rock passes over it under its own weight, shown in Figure 6. Low stress abrasion primarily occurs as cutting or fracturing depending on the geological content. Impact is typically not an issue in the low stress abrasion system, so material toughness is not of great importance. The most important material properties are hardness and cost.

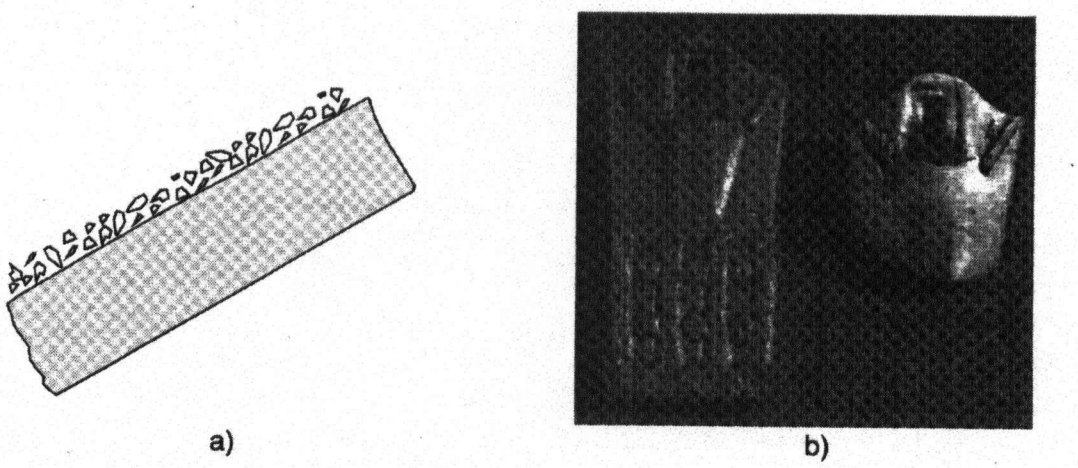

Figure 6: Low stress abrasion; a) rocks flowing down a chute and b) a new and a used tooth from a shovel (Llewellyn, 1996).

High Stress Abrasion

High stress abrasion imparts enough pressure on the abrasive to break it. It occurs in undercarriages of tractors, open gears and drag chains, shown in Figure 7. Wear rates are related to the ratio of material to abrasive hardness. Therefore, materials harder than

the abrasive hardness, should be used in this system. Figure 10 demonstrates the relationship between material and abrasive hardness. In addition the high stresses will impose large forces on the wear material requiring good material toughness properties to reduce wear and prolong the life of the component (Llewellyn, 1996).

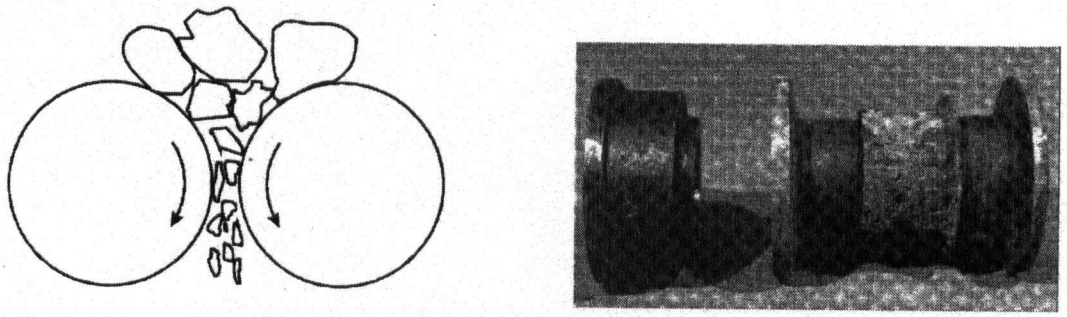

Figure 7: High stress abrasion; a) rocks being comminuted through a roller crusher and b) half new (left) and worn (right) roller for a tractor undercarriages (Llewellyn, 1996).

Gouging Abrasion

Gouging abrasion will deform the microstructure of the component up to a couple of millimeters from the surface. This type of abrasion imparts the largest amount of stress on the wear material and occurs mostly in primary and secondary crushers. Gouging abrasion is demonstrated in Figure 8. Most of the wear is caused as a result of plastic flow as large lumps of abrasive are driven into the wear component plowing out the wear material. This area of abrasion is the topic of this thesis and remedial measures will be discussed in detail in the following chapters (Llewellyn, 1996).

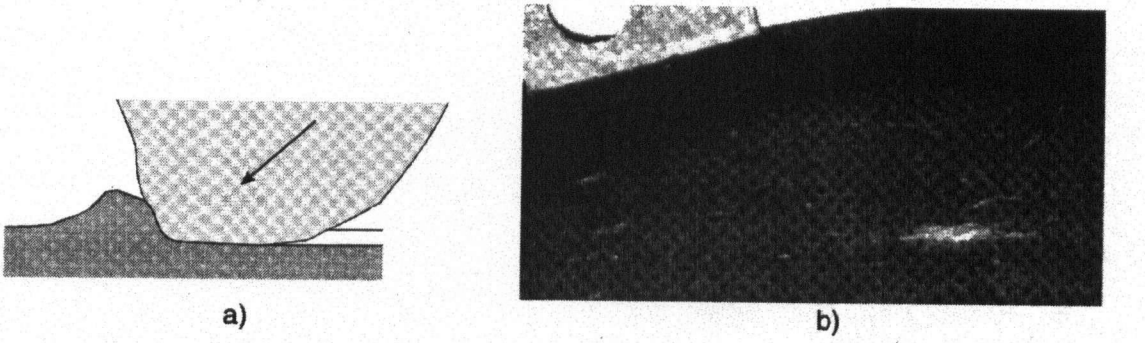

Figure 8: Gouging abrasion; a) Schematic of a jagged piece plastically deforming a wear material and b) a worn crusher mantle (Llewellyn, 1996).

Erosion

The other major wear mechanism encountered in the mining industry is erosion. Erosion is not considered as a "main" wear mechanism but has shown to be very prevalent and damaging in the mining industry and often occurs in combination with corrosion (Llewellyn, 1996). Erosion occurs when a dense concentration of particles transported in a fluid or gas impact or slide against a wear surface and is shown in Figure 9.

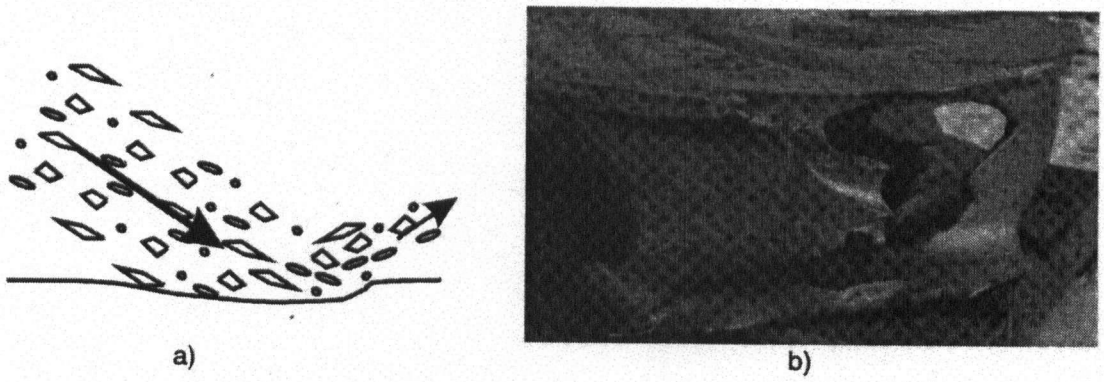

Figure 9: Erosive wear; schematic showing erosion and b) eroded slurry pump (Llewellyn, 1996).

Material properties that would reduce erosive wear are dependent on the angle of impact of the fluid/gas. Micro-cutting is the prevalent material removal system for low impact angles, requiring a material with high surface hardness. At high impact angles, micro-fracture becomes the dominant material removal method. Good material toughness will reduce micro-fracture. The combined effect of erosion/corrosion is greater than the individual components.

2.2.2 Abrasive Characteristics

According to geologists, minerals can be characterized by different factors; their mineralogical content, their grain size and their color (British Columbia Ministry of Energy and Mines, 2004). Geotechnical engineers categorize rocks according to their mechanical properties; such as Young's modulus, Poisson ratio, tensile strength, unconfined compressive strength and shear strength (Conduto, 2003). Evidently there are many different ways to classify a rock group, depending on the information required. It is common when dealing with wear to classify rocks by their mineral content to estimate particle angularity (Stachowiak, 2001). In the author's opinion particle angularity is an important abrasive characteristic, but a knowledge of the mechanical properties of the rock group also influences the amount of abrasive wear incurred, particularly when estimating abrasive wear in primary crushers where there are larger pieces of rock to comminute. Other abrasive characteristics that are sometimes taken in to consideration include the size of the feed and the size of the product (Utley, 2002).

Abrasive wear is occasionally defined by the surface hardness of the two interacting materials. For mining, the two interacting surfaces are the minerals and the

wear parts. Figure 10 is a comparison between the hardness of the abrasive, the hardness of the wear material and the amount of abrasive wear. As is shown, if the ratio of hardness is less than 1 (i.e. the hardness of the wear material is larger than that of the abrasive) then there are reduced wear rates. Increasing the ratio above 1 shows a drastic increase in wear. One thing to note is limited reduction in abrasive wear by using a hardness ratio smaller than 1 or larger than 1.2. This curve was originally generated from abrasive wear data for metals, but it is assumed that a similar principal is applicable to other wear materials (Llewellyn, 1996). Figure 11 compares the hardness of different minerals and the hardness of different constituents (ASTM, 2004).

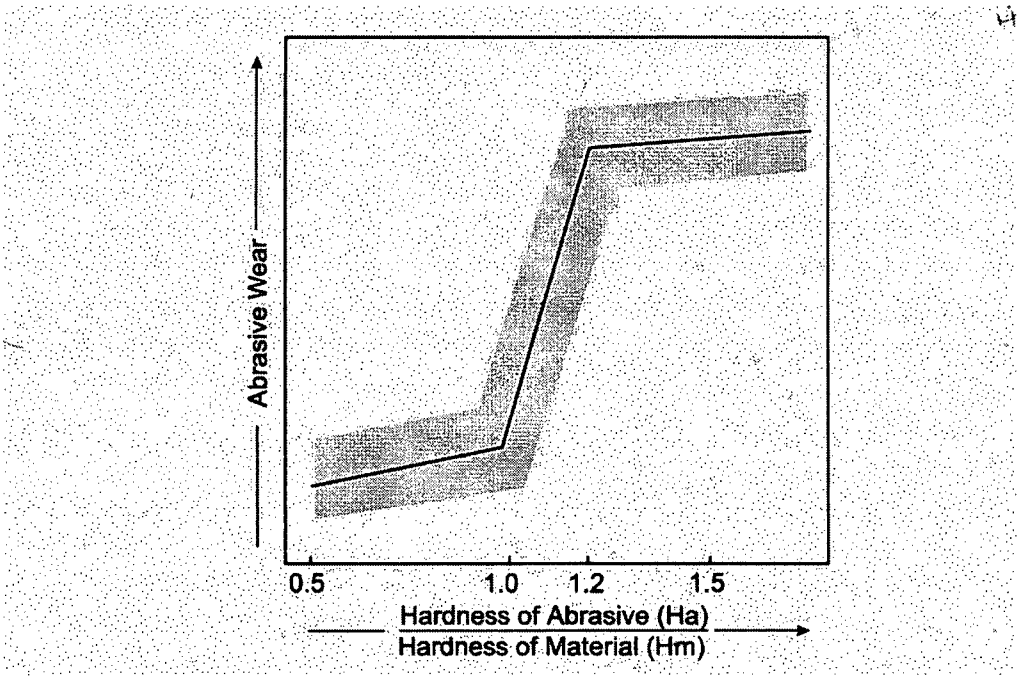

Figure 10: Relationship between abrasive wear and the ratio of material and abrasive hardness (Llewellyn, 1996)

Some work has been done on comparing the wear rates of different ores in field tests. Typically, the ores with the higher silica content give higher wear rates (Tylczak, 1999). Other research has shown taconite to increase wear rates (Wear Control Handbook, 1980). Particle angularity has been shown to be influential in the amount of

abrasive wear. Different factors have been proposed to quantify particle angularity with a numerical descriptor including the Spike parameter quadratic fit (SPQ), the roundness factor and the Invariant Fourier Descriptors (Stachowiak, 2001). Another attempt at a numerical descriptor of minerals includes the rock abrasive index (Beste, 2004). Because of its angular shape, quartz has been shown to have the largest influence on abrasive wear (Stachowiak, 2001);(Beste, 2004).

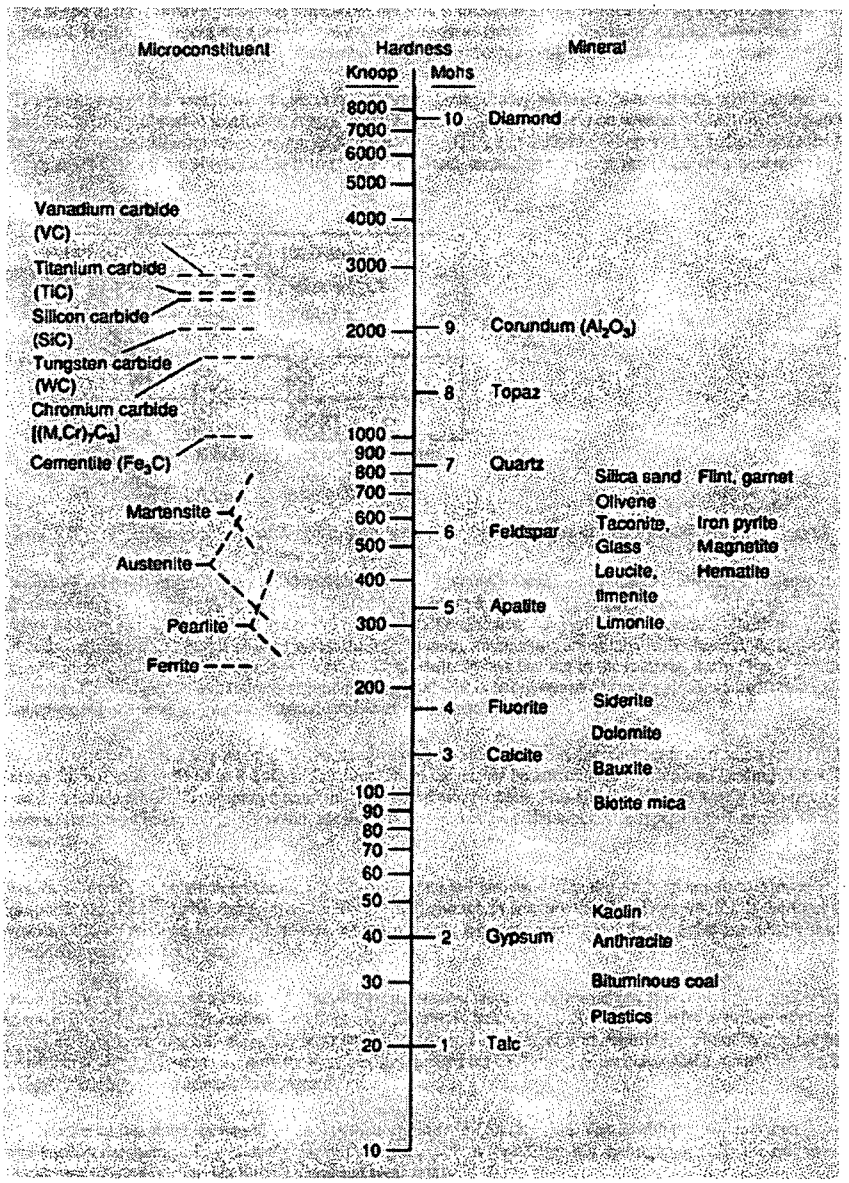

Figure 11: A comparison of surface hardness' for metal matrix constituents and commonly found minerals (ASTM, 2004).

2.2.3 Wear Materials in the Mining Industry

Wear materials in the mining industry can be broken up into five main groups; irons and steels, surfaced engineered, elastomers and plastics, ceramics and cermets and composites. The selection of the proper material for each situation depends on an understanding of the wear mechanisms present and choosing the material with the most

appropriate properties. Other important parameters that must be taken into account include the cost of the material and its workability (Llewellyn, 1996).

Irons and Steels

This group has a wide range of mechanical properties leading to a variety of surface hardness (~200HB - ~500HB), offering an assortment of solutions to wear problems in the mining industry. This group can be sub-divided into three main categories:

Pearlitic and martensitic steels: These steels typically provide moderate resistance to different types of abrasion, at an affordable cost. They are easily manufactured to suit the customer's service needs. As a result, the martensitic steels have found uses as shrouds and adapters on shovels and as mill liners.

Austenitic manganese steels: These steels are also cost effective. Although they have initial low surface hardness, they have phenomenal toughness and work hardening ability, allowing them to double their surface hardness. This makes these steels ideal in situations where there is a combination of impact and gouging abrasion, such as crusher mantles.

Abrasion resistant white irons: White irons are known to be very hard and brittle. They have high corrosion and abrasion/erosion resistant properties. However, they contain chromium, molybdenum or nickel that substantially increases their cost. To improve their toughness and allow welding installation, they have been successfully laminated to a mild

steel backing plate. Because of their increased impact resistance, these have found use as mill linings and skirting for buckets, hoppers and chutes.

Surface Engineered

Surface engineered materials are composed mainly as a high abrasion/erosion resistant coating placed on a base material selected for reasons other than its wear resistance. Surface engineered materials attempt to combine hardness and toughness to create the best possible wear plate. They are hardened through one of many surface heat treatment processes, or are given a harder surface coating. Two of the more common surface engineered materials are chrome carbide and tungsten carbide overlay; each material derives is abrasion/erosion resistance from the hard carbides found in its matrix. Typically these materials are placed on a steel backing plate. Because of their high surface hardness (>700 HB) they are used in high stress, sliding type abrasion situations such as digger teeth and bucket lips.

Elastomers and Plastics

Theses materials occupy a specific niche in materials that resists wear in the mining industry. The elastomers comprise mostly off-road tires, conveyor belts and haul truck box linings. The ASTM defines elastomers as a material that can be stretched to more than twice its length, then return quickly to its original length, at room temperature. Plastics were mostly used as epoxy resins and as pipes in pumping application because of their light weight. Both elastomers and plastics are known for their corrosion resistance, toughness and ease of fabrication. They rely mostly on their elastic properties for their wear resistance. Their main drawback is their unsuitability in gouging and tearing wear applications.

Ceramics and Cermets

These materials have a very high abrasion resistance at low and high temperature. Their main disadvantage is their lack of toughness. Concrete is considered to be a ceramic; therefore most properties associated to concrete can be applied to ceramics (strong in compression, weak in tension, superior corrosion protection...). Cermets are a combination of metals and ceramics. The most popular cermets are the cemented tungsten carbide found on drill bits. These carbide bits are selected because of their high hardness (~2000 HV).

Composite Materials

These usually are combinations of ceramics and epoxy resin or elastomers. Their main advantage is applicability and ease of use. They can prolong the life of a wear component until a scheduled replacement. However, they are also expensive and sometimes during their set time, the epoxy matrix can be worn, thereby severely limiting the resins wear performance.

2.3 Research into Wear in the Mining Industry

Abrasion is the dominant wear mechanism found in crushers and mills (A Strategy for Tribology in Canada, 1986) and research and literature available on abrasive wear is extensive. There are different paths available to follow towards the ultimate goal for understanding how abrasive wear occurs and how to reduce its impacts. In general, research into crusher wear follows three paths; theoretical, statistical and metallurgical.

2.3.1 Theoretical Approach

Researchers have successfully used very simple relationships that rely on basic physics principals such as the Archard's wear equation in addition to more complicated

stress/strain models and finite element modeling to explain the phenomenon of wear. In addition energy consumption of a comminution process has been successfully related to the amount of wear from said process.

Wear in crushers/mills is caused by breaking rocks; therefore understanding how a rock breaks would make it possible to design a more efficient machine to break it. Rock is a brittle material and will tend to break along a tension crack. Research is aimed at understanding "the formation and propagation of these cracks" (Donovan, 2003, pg 4). Griffith's brittle crack theory has been used to help explain particle fracture. In its most general sense, Griffith's theory states that there are stress concentrations at the tip of an existing crack allowing it to propagate outward. Modifications to this model have accounted for the existence of plastic deformation at the crack tip (Donovan, 2003). Different methods have been used to understand particle fracture. Finite element single-particle and inter-particle breakage models have been proposed to help understand the fundamentals of rock breakage (Tang, 2001a). Single-particle breakage is simpler to model because the contact forces are simpler. They come from only one direction, the "crushing plate". Inter-particle breakage is more complex as a result of the contact forces coming from random directions and random intensities (Tang, 2001b). Other considerations in the theoretical understanding of particle fractures include plastic and elastic deformation, the influence of particle size on crushing energy requirements and the particle failure mode (Tang, 2001a).

To help explain the extend of volume loss during wear i.e. the wear scars, Archard developed an equation that relates the total volume loss due to sliding wear to a "wear coefficient", the total distance of sliding and the normal load at contact. The relationship was originally developed for adhesive wear, but has found uses in abrasive wear analysis (Linquvist, 2003). This relationship is particularly useful in simple tribo-meters like the ball cratering or the micro-scale abrasion test where the abrasive has a uniform size and geometry (Trezona, 1999).

Researchers have also attempted to explain wear through energy consumption in the comminution process. Bond's work index (Third Theory of Comminution) has successfully been used to estimate the energy consumption of a crusher/mill. It relates the size of the feed and the size of the product to the energy required to make such a size reduction. With energy and wear being proportional; the more energy required by the system, the higher the wear of the system (Hawk, 1999). The main drawback of this theory is the motor. For the Bond's Work Index to be true, an accurate knowledge of the power draw and the efficiency of the motor is required. As a result the work index has to be setup for each individual grinding or crushing machine (Deniz, 2003).

2.3.2 Statistical Approach

On a macroscopic level, research relies on established empirical models to explain the impacts of wear. Initially, wear models were very simple and followed the age dependent failure mode. These models accepted wear as a factor, but were not concerned with the wearing process (Mercer, 1961). In addition, some shock models using probabilistic theories have also been used to explain the wearing process (Esray, 1973).

More recently research is aimed at using reliability models to reduce the impacts of wear by replacing worn parts before they adversely affect the efficiency of the machine (Park, 1988a);(Park, 1988b). Process models have been proposed to estimate ball mill wear as a factor influencing mill efficiency by using derived equations relating adhesive and abrasive wear to rate of energy used (Radziszewski, 1997).

2.3.3 Materials Approach

The materials approach to abrasive wear research typically involves testing wear materials in a laboratory tribo-system and then ranking them according to a weight or volume loss formula. In addition, the microstructure of unusual results is sometimes viewed (Bednarz, 1999). Extensive research has taken place understanding the fundamentals of abrasive wear. Many different laboratory tests have been designed to investigate different properties of wear materials, the abrasive or the way the abrasive interacts with the wear material. Extensive metallurgical literature exists explaining the wear resistance of different materials (Sare, 1997);(Marks, 1976);(Gore, 1997);(Qian, 1997);(Watson, 1980). Researchers have focused most of their attention on the testing and evaluation of different variations of white irons, manganese steels and different structural steels. Typically, they utilize a high-stress and a low-stress abrasion test to rank the material for its resistance to abrasion (Bednarz, 1999); (Tylcak, 1985); (Dodd, 1979); (Borik, 1972). There is little research into the performance of hardfacing or overlay materials in gouging abrasion situations (Llewellyn, 2004c).

Abrasive Wear Tests

The study of abrasion resistant materials is complex. Abrasion can be present in very small forms similar to adhesion; causing surface scouring or it can be present with

enough force to severely damage the surface of a wear plate through spalling and gouging (Burwell, 1957);(Rabinowicz, 1995). To study the abrasive resistance of materials, three different ASTM approved laboratory tests have been developed; Pin-On-Drum (G132), Jaw Crusher (G81) and the Wet (G105) or Dry (G65) Sand Rubber Wheel tests (Hawk, 1999); (Tylczak,1999). In addition to the three tests mentioned, the ASTM subcommittee on abrasion resistance is studying six additional tests to add to the list (ASTM, 2004). While these tests model one form of abrasion accurately, their relationship to field conditions is questionable. The full scale test is more representative, however it is also costly, difficult to control and time consuming to perform. As well, test material inhomogeneity is a concern during full scale tests (Tylczak, 1999);(Hawk, 1999).

The laboratory tests can be broken up into the different classification systems mention in section 2.1.2. For the purposes of this thesis, the tests will be termed according to the load placed on the abrasive.

Low Stress Abrasion Test

The Dry Sand Rubber Wheel Test (DSRW) is a three-body, low stress abrasion test. The test consists of a wheel that is spun while a specimen is pressed against it. Figure 12 shows a typical DSRW test setup. At the contact point between specimen and wheel, sand is inserted as the abrasive particle. The test can be varied at two points; the distance the specimen travels on the wheel and the load that is placed on the specimen. The ASTM has recognized four different procedures and setups possible for this test (ASTM 2004b). The specimen tested is 25 x 75 mm in size and is 3 to 13 mm thick. The

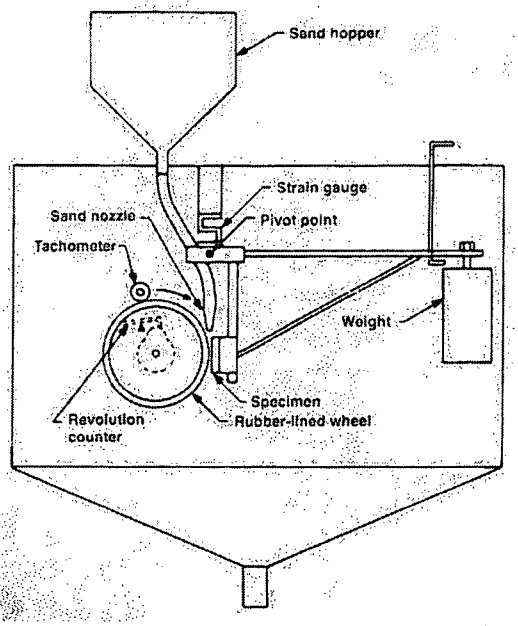

Figure 12: Schematic of a Dry Sand Rubber Wheel test apparatus (Hawk, 1999).

intent of this test is to relate low stress abrasion that one might encounter in linkages, pivot pins and wire ropes. This type of abrasion allows the sand particle to both slide and roll along the specimen. The results are reported as a wear factor measured according to volume lost. Variations on the test include using a steel wheel instead of a rubber wheel and using wet instead of dry sand (Wirojanupatump, 1999).

High Stress Abrasion Test

The Pin-On-Drum (POD) test is a two-body, high stress abrasive test and its setup is presented in Figure 13. The specimen is machined to a diameter of 6.35 mm and is 20 to 30 mm long. Like the stylus on a record player, the pin is moved over a drum coated with an abrasive paper. A normal load of 66.7 N is applied to the pin. The drum is rotated as the pin is pushed against the abrasive cloth. The position of the pin is moved along the axis perpendicular to the motion of the drum. This allows the pin to encounter fresh cloth with each revolution. Typically an abrasive cloth consisting of Al_2O_3 or SiC

is used to cover the drum. The wear resistance is evaluated as a wear factor in relation to a reference material and is measured according to weight loss. The Pin-On-Drum test has been used to evaluate the wear resistance of materials since 1910. As a result, there are many variations to the test and the test procedure. This test simulates the wear encountered during grinding (Hawk, 1999).

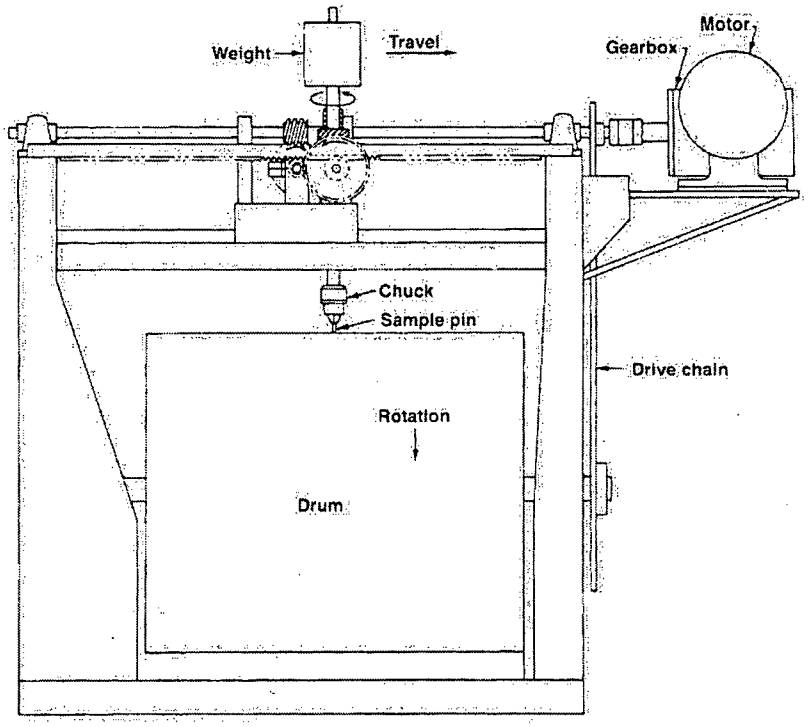

Figure 13: Schematic of a Pin-on-Drum test apparatus (Hawk, 1999).

Gouging-Abrasion Test

A laboratory-sized jaw crusher (152 mm by 101 mm, 4"x6") is used to relate gouging resistance of wear materials. Gouge is defined by the Merriam-Webster's dictionary as a verb "to scoop out". Therefore the term gouging defines the removal of material from the surface of the wear plate. The jaw crusher test is a high stress, three-body abrasion test (Moshgbar, 1994);(ASTM, 2004). It is also defined as the Gouging Abrasion test. The motion of the rocks as they are being crushed (rolling or sliding; two

or three-body abrasion) causes the difficulty in categorizing what type of abrasion this test represents. Evidence from the abrasion scars on the wear plates suggest that they both roll and slide (Hawk, 1999). Figure 14 shows a typical jaw crusher testing apparatus. The crusher's jaws are replaced with a set of test and reference plates. The plates are 230 mm by 83 mm and typically 19 mm thick, although the thickness can vary. They are positioned in the crusher opposite each other. The reference plate on the moving jaw faces the test plate on the stationary jaw and vice versa. The test is run with up to 910 kg of a known abrasive sent through the jaws. The plates are then removed and weighed. The wear on the plates is represented as a wear factor, a ratio of the weight lost on each plate. Variations on the test procedure can include different wearing material, the amount of wearing material and the make up of the test plates (Hawk, 1999); (Liang, 2004). With the increased use of hard overlay materials, volume loss is occasionally used to calculate the wear factor (Llewellyn, 2004c).

There are additional variations to the Gouging Abrasion test procedure. If the test program is extensive, a statistical variation of plate location can eliminate the use of the reference plate and reduce the overall number of tests (I.R. Sare, 1997). The abrasive and the amount of abrasive can also be varied (Llewellyn, 2004c).

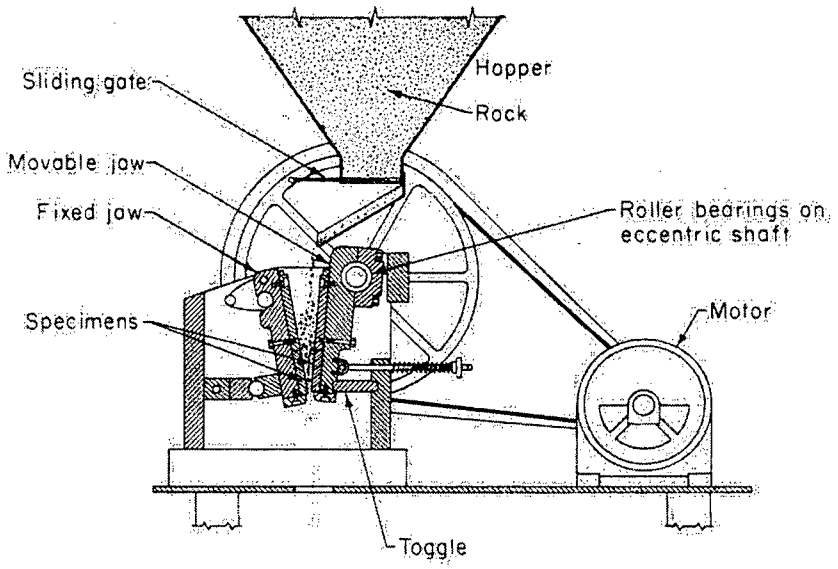

Figure 14: Schematic of a Jaw Crusher test apparatus (Hawk, 1999).

Other Wear Tests used in the Mining Industry

Other tests that are used to evaluate wear in the mining industry include the impeller tumbler test and various field scale tests. Each field scale test is used to model a specific area of wear in mining. The impeller-tumbler test was developed to simulate the wear encountered during impact of crushing bars, it models impact abrasion.

The impeller-tumbler test apparatus is shown in Figure 15. The apparatus can accommodate test plates that are 75 x 25 x 12.5 mm. The test procedure includes four installments of 600 g of high silica quartz. Each batch of "ore" is placed in the tumbler at fifteen minute intervals. At the end of the one hour test, 2.4 kg of "ore" has been processed. The end result is a wear factor relating the grams lost in the wear plate to the kWh of energy used (Hawk, 1999).

The best abrasion test to perform is a field wear test (Tylczak, 1999);(Hawk, 1999). By placing the test materials in service conditions, it is possible to view its actual behavior and occasionally no interpretation of the results is necessary (i.e. when comparing the wear from teeth on a shovel). However a field analysis is time consuming, expensive and difficult to control. Success has been had when comparing simple wear mechanisms (two body, low stress abrasion) encountered in the field with laboratory wear tests that produce the same simple wear mechanisms. However, results are not so promising when comparing more difficult wearing mechanism (three body, gouging abrasion) (Hawk, 1999).

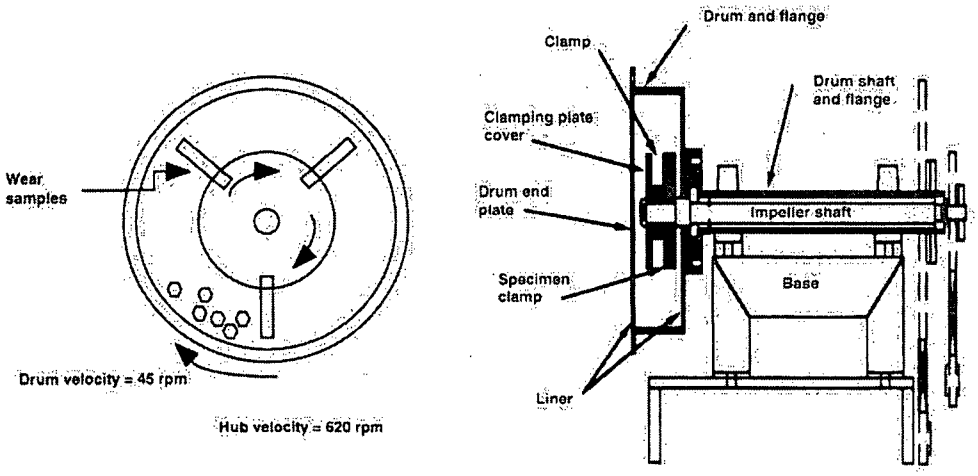

Figure 15: Schematic of an Impeller-Tumbler test apparatus (Hawk, 1999).

Data Analysis

The results for the previously described tests can be analyzed in different ways. Relationships between surface hardness and wear factor have been developed in attempts to predict the wear rate of a material (Bednarz, 1999); (Hawk, 1999); (Tylack, 1999). In general, the result from the pin-on-drum test and the dry sand rubber wheel test (for similar materials i.e. monolithic, abrasion resistant, quench and tempered steels) is a plot of surface hardness vs. wear factor that is shown to be linear. However not all abrasion

tests reveal such a simple relationship. The gouging abrasion test tends to show a decreasing wear factor until a certain surface hardness and afterwards the wear factor is relatively constant. The impeller-tumbler test does not reveal any specific relationship (Hawk, 1999); (Tylczak, 1999). Further complication arises in discussing the gouging abrasion test results when attempting to determine at which surface hardness the wear factor becomes constant. Research has shown it to exist at approximately 450 HB and at approximately 250 HB. (Bednarz, 1999);(Hawk, 1999). In attempting to rank materials before testing, the surface hardness may prove to be a good indicator of abrasion resistance. However, with certain materials such as manganese steel that have the ability to work harden, the initial surface hardness indicator is not as accurate. In addition recent work has shown that at higher surface hardness, the microstructure has a greater influence on the gouging abrasion resistance of a wear material, than the surface hardness itself (Llewellyn, 2004b).

With the increased use of tungsten carbide hard coating overlay materials, traditional wear factor relationships are no longer valid (Llewellyn, 2004c). These are being used increasingly (WC) on teeth and plates in breaker and sizer systems. When rated using the gouging abrasion test, the WC overlay has an extremely poor performance. However, the tungsten coating is based on a nickel alloy and the density of the nickel is approximately half that of the tungsten. Therefore the traditional measure of wear factor from the gouging abrasion test relating the weight loss of the wear plates puts the WC overlay at a disadvantage. A more suitable comparison is the volume loss of the plates and it will be discussed in section 3.3.4.

2.4 Literature Review Summary

Abrasive wear is costly to the mining industry. Researchers have long realized the need for a systematic approach to understanding the behaviour of materials, abrasives and comminution systems.

There are presently many options and tools available to the researcher in pursuit of the goal of understanding wear. The path can be either completely theoretical, understanding the fracture mechanics of a naturally occurring abrasive; experimental, trying to design a wear test that is gives results of sufficient quality as to relate to field observations; or the researcher can choose to improve on the existing body of knowledge already in use in process control and comminution circuit design.

There are many factors that influence a materials abrasion resistance including the type of wear material matrix used and characteristics of the abrasive. The quartz content of the abrasive has shown to be very influential in abrasive wear because of its angularity and hardness. Also taconite has been shown to be very abrasive.

Abrasive wear research has focused on the metallurgical aspect. Different wear tests have been developed to help understand and explain the different wearing mechanisms. Unfortunately the main wearing mechanisms are normally present in combination with each other, making understanding the abrasive wear process difficult. Traditionally gouging abrasion resistance is measured as a wear factor; a ratio of mass or volume loss of a test and a reference material. Previous research has focused on testing various formulations of white iron, manganese steels and abrasion resistant steels. This

work will add the existing gouging abrasion knowledge of standard AR steels and CrMo white irons. In addition it will test hypereutectic white irons (laminated and cast form) and chrome carbide and tungsten carbide overlay material in gouging abrasion situations.

3.0 Materials and Procedures

The following sections describe the equipment setup to facilitate the procedures used to test and analyze the wear materials for this work. The testing procedures closely follow the procedures set out in the ASTM G81 Gouging Abrasion test. Modifications to the procedure will be outlined in section 3.2. The testing was completed with the laboratory jaw crusher in the Coal and Mineral Processing Laboratory at the University of British Columbia. The analysis was done at the National Research Council Laboratory in Vancouver, British Columbia.

3.1 Materials

Different wear materials were tested in gouging abrasion conditions. One wear material (AR500 Steel) was tested with different abrasives. This section will describe the wear materials and the abrasives used.

3.1.1 Wear Materials

Fifteen different wear materials were tested and analyzed using the procedure described in this section. They represent the range of materials used in the oil sands with increasing interest in gouging abrasion properties. They are listed in Table 4. The manganese steel plate is not in service presently, but was included in the series of tests to establish its work hardenability under such large contact stresses and it is a standard material for crusher mantles.

Table 4: Reference and test plate materials.

Class	Type / Ident.	Thick. -mm	Hardness – HB	Description
Rolled reference steel	Q &T 100	19.05	240	ASTM A 514 Grade B structural steel
	Q &T 100	25.40	232	ASTM A 514 Grade B structural steel
Rolled AR steel	AR 400	19.05	384	CMnB abrasion resistant (AR) steels. Quenched and tempered to various nominal hardness levels
	AR 450	19.05	390	
	AR 500	19.05	462	
	AR 600	19.05	552	
Austenitic Manganese Steel	MnSt	19.05	205	Solution treated ASTM A 128 Grade A
White iron castings (WCI)	CrMo WI	19.05	730	ASTM A532 11B (15%Cr3%Mo3%C)
	Hyperchrome®	19.05	710	Proprietary hypereutectic high Cr
Laminated white iron plates	Laminite	25.4	755	ASTM A532 11B (15%Cr3%Mo3%C) WCI brazed to a steel backing plate
	Laminated Hyperchrome®	19.05	640	Proprietary hypereutectic high Cr WCI brazed to a steel backing plate
White iron /rubber laminate	Rubbadex	25.4	750	ASTM A532 11B (15%Cr3%Mo3%C) WCI bonded to a rubber /steel layer
CrC weld overlays	CrC SOL	25.4	564	6.4 mm thick single pass ~30%Cr 4%C bal. Fe deposit.
	CrC DOL	25.4	595	9.6 mm thick, double pass ~30%Cr4%C bal. Fe deposit.
Tungsten carbide overlays	WC 1	19.05	478	4 mm thick 60Wt.%, cast and crushed (eutectic) WC in a 50HRC nickel alloy matrix.
	WC 2	19.05	397	4 mm thick 60Wt. % macrocrystalline (monolithic) WC in a 30HRC nickel alloy matrix.
	WC 3	19.05	491	4 mm thick 60Wt.% macrocrystalline (monolithic) WC in a 50HRC nickel alloy matrix.

Each of the different classes of material listed in Table 4 derives their wear resistance from different sources from different features as described below.

Abrasion Resistant (AR) Steels

These materials are known for their cost effectiveness and moderate wear resistance. Their abrasion resistance comes from the microstructure of tempered martensite. Theses AR steels are alloyed with carbon and minimal amounts of boron (0.002%-0.005%) both of which affect the hardenability of the wear plate (Llewellyn,

2004b). The surface hardness prior to installation of these wear plates is normally indicative of its abrasion resistance. The AR600 plate is a new product on the market, which has not been previously tested.

Austenitic Manganese Steel

Like the AR steels, the austenitic manganese steel derives is abrasion resistance from its microstructure. However, unlike the AR steels its initial surface hardness is not indicative of it wear performance. The austenitic manganese steels are known for their work hardenability and extreme toughness as previously mentioned in section 2.2.3 The austenitic manganese steel was chosen to view its cold work hardening under the high contact stresses encountered in the gouging abrasion test.

Cr and CrMo White Iron Castings

These multiphase materials obtain their abrasion resistance from a combination of matrix hardness and high (M_7C_3) carbide hardness. These plates are characterized by the Carbide Volume Fraction (CVF). As the CVF increases, then theoretically so does the abrasion resistance. The wear plates tested are hypoeutectic CrMo white iron containing chromium (~15%) and molybdenum (~3%) and the recently developed hypereutectic Hyperchrome white iron, which has chromium levels greater than 30%. Previously, white iron castings were only available in the hypoeutectic form as the hypereutectic version was too brittle to be cast properly. A hypereutectic white iron casting (and laminate) was obtained for this work. Figure 16 is a schematic of the FeCr(30%)C phase diagram which describes the microstructures of the two white iron castings. The hypoeutectic material derives its abrasion resistance from primary alpha (austenite) dendrites and eutectic carbides in a

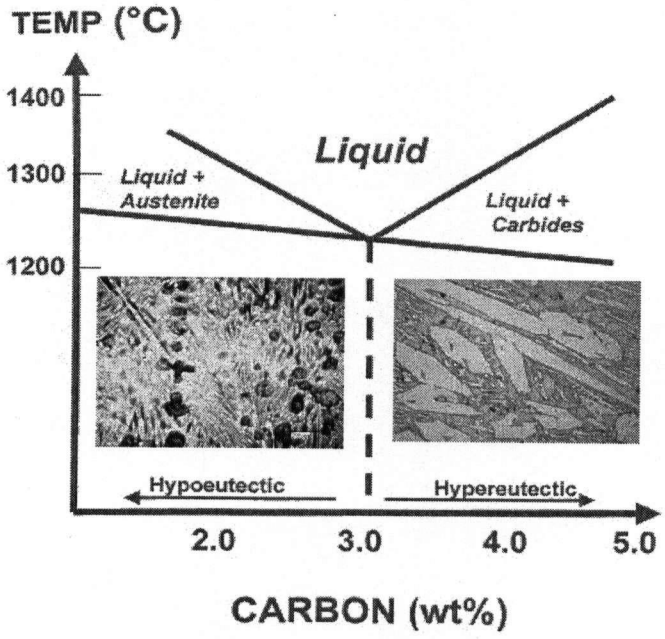

Figure 16: Schematic FeCrC liquidus diagram (Llewellyn, 2004b)

martensitic matrix. The hypereutectic (Hyperchrome) material draws it abrasion resistance from primary M_7C_3 carbides. During solidification, the extra carbon and extra chromium in the system form the primary carbides and a martensitic matrix, where M is a composition of Fe, Cr, C and Mo. It is know that the hypereutectic casting would provide greater abrasion resistance by increasing the CVF of the wear plate. However with increased CVF comes decreased toughness, which affects the wear plate's gouging abrasion resistance during high contact stresses (Llewellyn, 2004b). It has been successfully used in pumping applications in the mining industry (Llewellyn, 2004a).

Laminated White Iron Plates

To increase the toughness of the white iron castings, they were laminated to a structural steel backing plate. This arrangement allows the wear surface to maintain its high CVF while the backing plate gives the wear plate increased toughness and

workability (Llewellyn, 2004b). The Rubbadex wear plate contains a 5 cm ($^1/_4$ inch) rubber layer between the white iron and structural steel backing plate. It was tested to see if the rubber decreased the noise caused during comminution and if the rubber helped reduce damage caused by impact/indentation seen in some crushing situations.

Chrome carbide weld overlay wear plates

The constituents of the chrome carbide (CrC) weld overlays are the same phase diagram shown in Figure 16. The CrC weld overlay plates have an increased carbon content to make them harder. With increased carbon content, there is an increased CVF and a decrease in the toughness of the material. For this reason the CrC weld overlay plates are present as hardfacing layers on selective wear components, generally 5-10 cm thick. Like the hypereutectic white irons, the CrC overlay plates rely on their primary M_7C_3 carbides for their abrasion resistance. The increased chromium and carbon of the CrC overlay plates generally leads to cracking of the hardfacing during solidification. This has shown not to have any influence on the abrasion resistance performance of this material (Llewellyn, 2004b).

Tungsten carbide/nickel based alloy overlay plates

These materials rely on the hardness of their primary tungsten carbides (WC and/or W_2C) for their abrasion resistance. The carbides can be found typically in a nickel-chromium alloy binder. While the primary carbides are a different composition than those found in the CrC overlay plates, the tungsten carbide plates also use the CVF as a measure of the abrasion resistance of the wear plates. Typically a higher CVF results in

greater abrasion resistance. In addition the carbides are susceptible to heat treatment; therefore special binding techniques have to be used to join the hardfacing to the backing plates without detrimental affects to the primary carbides. The materials tested in this thesis are deposited with Plasma Transfer Arc Welding. It has been reported that this method has the least impact on the primary carbides and gives low dilution rates between the hardfacing and back plates (Llewellyn, 2004b).

3.1.2 Abrasives Types

In an attempt to correlate wear to rock type, three different rock types were crushed. The test plates were made of the same AR500 steel for all three materials. They were selected because of availability. Two types were waste rock obtained from the Highland Valley Copper (HVC) mine and the third was an aggregate obtained from a local quarry. The abrasive supplied by HVC was screened to be sized between 25mm and 10mm diameter. The aggregate was screened to be between 20mm and 14mm. Their quartz content was measured using a phase analysis test. The complete results from the test can be seen in Appendix 1.

Table 5: Quartz content for the different rock types crushed.

Abrasive	Quartz Content (%wt)
Valley (HVC)	48.6
Lornex (HVC)	31.5
Aggregate	7.2

3.2 Test Setup and Procedure Modifications

The ASTM provided a basis for the procedures used to test the wear plates. The standard G81 procedure set out by the ASTM is designed to help a researcher setup a brand new jaw crusher. The laboratory jaw crusher at UBC was already setup; as a result

logistical differences exist between the described ASTM procedure and the actual methods used. The ASTM procedures will not be repeated, only the major modifications will be explained.

3.2.1 Crusher Setup

The crusher is designed to comminute approximately 226 kg per hour. A schematic of the crusher can be seen in Figure 17. The stone is manually fed into a hopper that holds 136 kg. As the hopper emptied an additional 91 kg was put into the

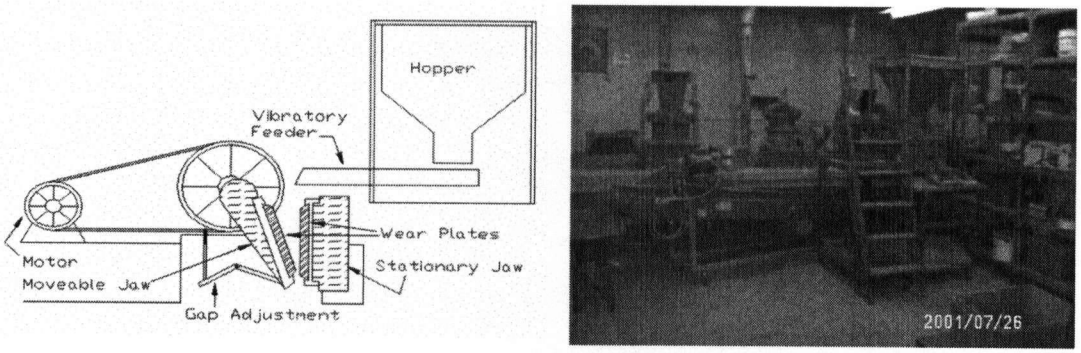

Figure 17: (Left) schematic of jaw crusher and (right) actual crusher setup.

hopper to provide the 226 kg. The wear plate installation, product gap and holder plates were checked at each 226 kg interval. The feed is directed into the crusher with a variable speed vibrating feeder. The variable speed allowed the operator to maintain a choke-feed condition reducing the indentation of the jaws. In addition, the lip of the feeder allows the operator to remove outside debris (such as twigs and garbage) from the feed before crushing.

The gouging abrasion testing was completed in two phases. The initial phase used 454 kg of rock and the second phase used 908 kg. The logic for this choice will be explained in section 3.2.2. For the first phase of testing, the crushed product was simply removed by sample bucket. However, for the second phase of testing, a less labor

intensive product removal method was required. A used conveyor system was modified to fit under the table holding the crusher. The modifications included building a new frame and installing a new motor. The frame was designed and built with Unistrut. With the conveyor working, the second phase of testing included more crushing with less labor. The current crusher setup can be seen in Figure 17.

There are two main differences between the UBC and the ASTM setups. The first difference is the amount of abrasive comminuted, which will be discussed in the next section (Section 3.2.2). The second difference is the way the abrasive is fed into the crusher. The ASTM setup has the hopper directly over the crusher. The UBC setup has a vibrating feeder feeding the crusher. The ASTM setup is easier to maintain choke feeding conditions, but the UBC setup is easier to stop during testing should there be a problem.

3.2.2 Testing Methodology

The first phase of testing consisted of steels and irons. Overlay and hardfacing materials were tested during the second phase of testing. The initial test performed involved removing and weighing the wear plates at each 226 kg up to 908 kg. The weight loss per plate per position vs weight-of-rock-crushed was plotted. As indicated in Figure 18, there is a relatively constant weight loss for irons and steels after approximately 227 kg of rock have been crushed (The test plate used during this trial is the cast CrMo white iron). This allowed the researchers to reduce the total amount of rock crushed from 908 kg to 454 kg, while still acquiring quality results. Since there is limited previous research into abrasive resistance of overlay and hardfacing materials, the second phase of testing comminuted 908 kg, as the ASTM recommends.

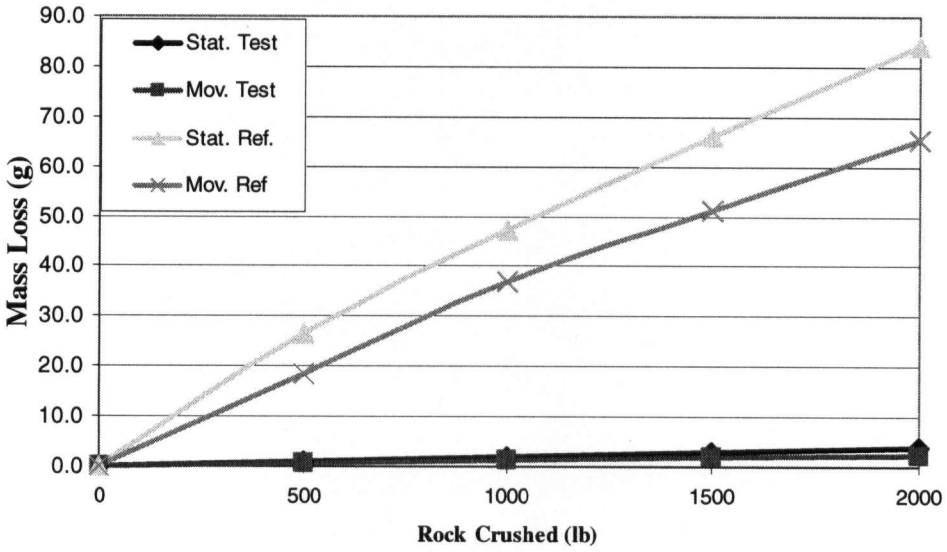

Figure 18: Constant weight loss for all four plates after approximately 750 lbs crushed.

3.3 Test Data Analysis

Section 4 contains the results of the testing program. The results will be presented in three different forms; microscopic correlation, wear factor and wear rates. All three forms are described in this section. The wear rates and wear factors will be used to rank the fifteen different test materials according to their gouging abrasion resistance. The microscopy work involves surface wear scar and microstructure evaluation. The surface wear scars and microstructures will be used to explain the different wear performances. The wear rates and wear factors will also be graphed against the quartz content of the different abrasives in an attempt to predict the wear life of the wear plates under gouging abrasion conditions.

3.3.1 Microscopic Analysis

To better understand the test behavior, certain plates were sectioned in order to view their post test microstructure. At the same time, small samples were taken from the

used test plate to examine the surface wear scars under a Scanning Electron Microscope (SEM). Table 6 is a list of the equipment and materials used during the cutting and mounting phase of the testing.

All of the tested wear plates showed the same area of increased attack, about 5 mm up from the bottom of the plate. The microscopy samples were taken from this area. The 230 mm x 83 mm plates were cut with an abrasive saw to fit the polishing mold (approximately 25 mm by 6 mm) and the SEM. After cutting, the samples were polished to a mirror finish and stored so as not to rust. Each microstructure sample was viewed and photographed with an optical microscope. The SEM samples were mounted with carbon paint to ensure conductivity.

Table 6: List of machines used to prepare and analyze the post test wear plates.

Action	Machine
Abrasive Cutting	Discotom 10" abrasive saw – 31 tre blade Microstar 2000 – Robocut 14" abrasive saw
Mounting and Polishing	Pneutmet II Mounting Press Struers Rotopol – 35 – 4 steps
Optical Microscope	Olympus- PMG 3 Leica Camera – IM50 Photo Manager
Scanning Electron Microscope	Hitachi S3500N Variable Pressure SEM
Microhardness Test	Buehler Microhardness tester 1600-3600
Surface Hardness Test	New Age Indentron

3.3.2 Wear Factor Analysis

The ASTM G81 test procedure suggests using a volume loss comparison to evaluate the wear factor for the test. For each test there is a reference wear plate and a test wear plate per jaw, for a total of four wear plates per test. Figure 19 shows the configuration of the wear plates for testing. The suggested evaluation method is to take the average volume loss ratio from the moveable and stationary jaws according to

Equation 1; where X_s and R_s is the volume loss for the test and reference wear plates from the stationary jaw and X_m and R_m is the volume loss for the test and reference wear plates from the moveable jaw. Completed detailed results are available in Appendix 2.

$$F = 0.5\ (X_s/R_s + X_m/R_m)$$

Equation 1: Volume loss ratio used to calculate the wear factor

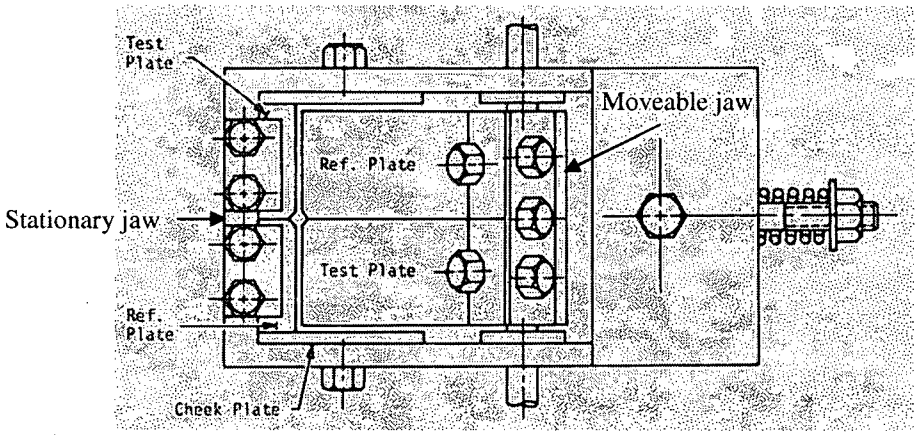

Figure 19: Wear plate location on the moveable jaw (right) and stationary jaw (left).

3.3.3 Wear Rate Analysis

The wear rates were calculated from raw data collected during testing. The mass losses were measured from the test plates. The volume losses were calculated using the appropriate densities as discussed in section 3.3.4. The wear rate (R) was calculated according to Equation 2; where R is the wear rate (mm^3/kg), V is the volume loss (mm^3) and A is the amount of abrasive used (kg). Complete detailed results are available in Appendix 3.

$$R = V / A$$

Equation 2: Equation used to calculate the wear rate of different materials tested.

3.3.4 Density Variation

Because of comparable densities, the mass loss is a suitable replacement for volume loss in equations 1 and 2 for the irons and steels tested. However the difference in density between the nickel alloy based matrix and the eutectic/monolithic carbides for the tungsten carbide material gave erroneous wear factors. The nickel alloy matrix has a density of approximately 8.4 g/cc, the eutectic carbide has a density of approximately 16.55 g/cc and the monolithic carbide has a density of approximately 15.6 g/cc. To correct this problem a nominal 60:40 weight ratio was used to calculate the density of the entire plate. The plate containing the eutectic carbides had an estimated density of 12.17 g/cc and the plates containing the monolithic carbides had an estimated density of 11.73 g/cc.

The nominal 60:40 weight ratio method for determining the plate density was confirmed using the High Stress abrasion test and laser profilometry. Test coupons of the same material tested in the jaw crusher, where tested using the High Stress Abrasion (HS) test. The weight loss was used along with the estimated densities to calculate the volume losses of the test coupons. A laser profilometer was then used to measure the actual volume loss of each test coupon. The two volume losses were then compared. Table 6 shows the comparison of the calculated and measured volume losses for the different tungsten carbide overlay materials tested in the HS test. There are four different alloys. All have the same nickel alloy based matrix.

Material	Calculated Volume Loss (mm^3)	Measured Volume Loss (mm^3)
1 pass S/F Eutectic PE 8213 **55% eutectic WC**	74.7	78.7
Multipass S/F Alloy St-66 Durit 5545/Eutectic PE 8217 (Blended) **60% eutectic** Wc/NiCrBSi	68.7	65.3
PTAW Durit 6050M **60% Monolithic** WC/NiBSi	50.2	53.2
PTAW SRW T058 **60% Eutectic** WC/NiBSi	42.2	42.8

Table 6: Calculated and measured volumes for PTAW WC material in the High Stress Abrasion Test.

4.0 Results

4.1 Wear Factor

The wear factors, presented in Figure 20, can be classified into three distinct groups. The groups are split according to the viewed microstructures and wear factors. The first group, containing all of the formulation of the CrMo white irons (laminated, cast and Rubbadex) and the double overlay chrome carbide (DOL), showed the greatest gouging abrasion resistance. These materials possessed hypoeutectic to eutectic microstructures. The second group, containing the proprietary Hyperchrome (hypereutectic) materials and the single overlay chrome carbide (SOL), had slightly higher wear factors while still displaying good gouging abrasion resistance. The second

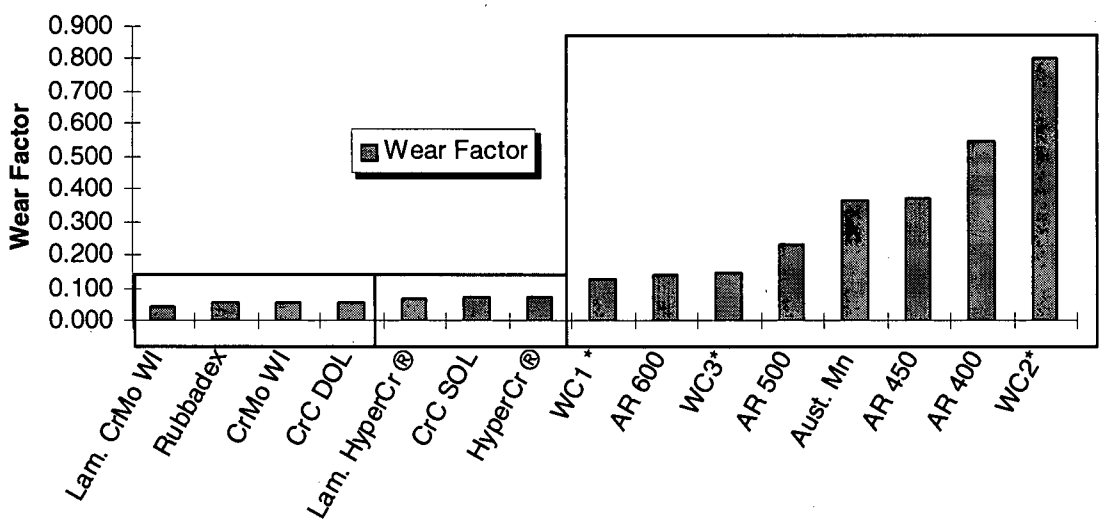

Figure 20: Wear Factor for each material tested in both phase 1 and phase 2. Star (*) indicates the wear factor is a volume based calculation.

group of materials contained hypereutectic microstructures. The third group contains the rolled quench and tempered steels, the various formulations of tungsten carbide overlays and the cast manganese steel. There is a little increase from the first to the second group,

from 0.056 to 0.078, but there is a larger increase into the third group whose wear factors are all greater than 0.1. The microstructure in the third group is either tempered martensite, work hardened austenite and/or WC/Ni based composites.

The laminate CrMo white iron had the lowest wear factor and therefore the best gouging abrasion resistance. The cast hypereutectic chromium white iron, in both the laminated and unlaminated form, demonstrated good gouging abrasion resistance with wear factors slightly higher than the CrMo white irons, however there was increased spalling from the hypereutectic plates. The abrasion resistance (AR) steels performed in accordance with their surface hardness. The AR600 steel was the best performer and the AR 400 steel had the highest wear factor. The manganese steel work hardened and had a similar wear factor to the AR 450 steel. As a result of its changing surface hardness, the manganese steel is not included in any discussions about surface hardness. The various formulations of the much more expensive tungsten carbide overlay material did not perform as well as expected. In fact, the formulation with the soft matrix and monolithic carbide (WC2) had the highest wear factor of all the plates tested.

4.2 Selected Post-Test Wear Material Microstructures

Selected test materials were sectioned in order to view their post test microstructures. The samples were all taken from the same general area on the test plates. Generally materials that rely on carbides for their abrasion resistance were examined. The CrMo white iron was compared with the Hyperchrome because they are both white irons with different microstructures. The Hyperchrome is a hypereutectic structure and the CrMo white iron is a eutectic/hypoeutectic structure. The SOL and DOL were also

compared in an attempt to explain the difference in wear factors. Of particular interest is the poor performance of the WC overlay materials, they were also sectioned and viewed in the SEM.

4.2.1 CrMo White Iron and Hyperchrome Microstructures

The microstructures from the first group displayed hypoeutectic and eutectic structures containing transformed primary austenite dendrites and eutectic carbides. For all the micrographs, the top of the figure shows the crushing surface.

Figure 21 is a micrograph of the typical surface microstructure of the best performing laminated CrMo white iron. The crushing surface is indented at the right-hand-side arrow resulting in deformation of both the eutectic carbides and surrounding matrix (left arrow). The carbides show no sign of cracking or spalling. In addition, the microstructure is finer, when compared to the hypereutectic structure displayed in Figure 22. The microstructure shown in Figure 21 is typical of the CrMo white irons (cast, laminated, rubbadex) tested in this work.

Figure 22 contains the microstructure seen in the laminated and cast hypereutectic test plates. The hypereutectic microstructure has a coarser structure compared to the CrMo white iron and contains large primary carbides. The high contact stresses in the gouging abrasion test have cracked theses carbides and they are in the process of spalling. This micro-spalling is not to be confused with the macro-spalling shown on the test plate in Figure 22. The macro-spalling results from the generally brittle nature of the material combined with the large contact stresses encountered during the gouging abrasion test.

These materials also tend to crack during solidification thereby providing the start point for macro-spalling. They do not influence the materials wear resistance during low stress abrasion (Llewellyn, 2004a). The micro-fracturing results in increased wear.

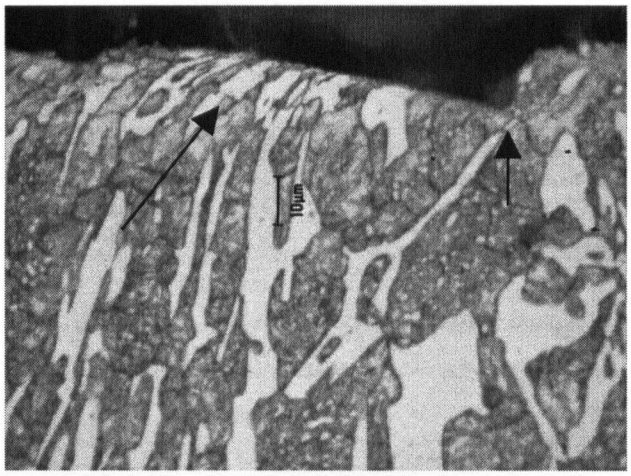

Figure 21: Eutectic structure of the laminated CrMo white iron. Eutectic carbides (arrowed) show signs of deformation, not cracking.

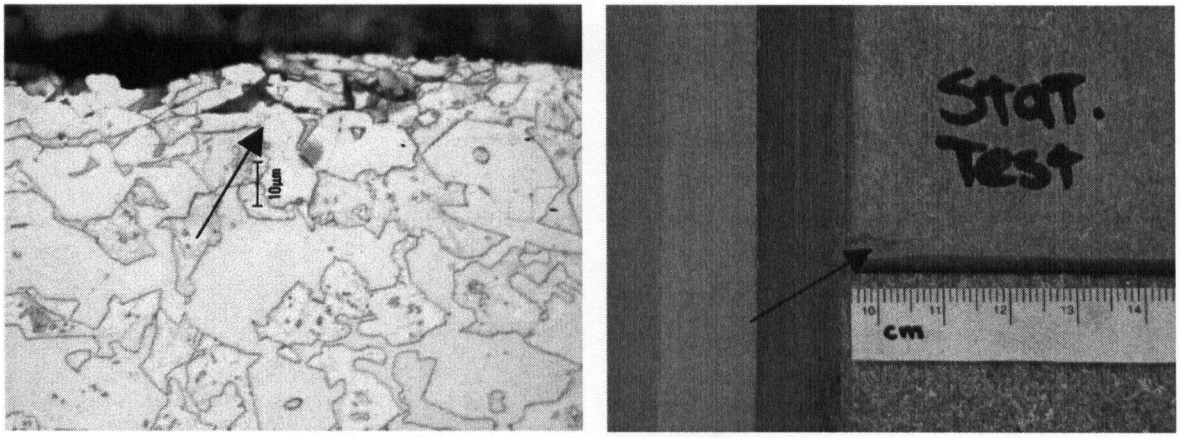

Figure 22: (Left) Hypereutectic structure with large primary carbides. Primary carbides show signs of micro-cracking and micro-spalling. (Right) Macroscopic edge spalling of the Hyperchrome material

4.2.2 Chrome Carbide Overlay Microstructures

The double overlay (DOL) chrome carbide material, ideally containing the same structure as the single overlay material (SOL), was one of the best performers. Figure 23 contains the micrographs of the DOL and SOL material. The micrograph of the DOL material shows it contains a slightly hypoeutectic structure with primary dendrites, while the SOL material contains a eutectic to hypereutectic structure with primary carbides. The larger, harder, more brittle primary carbides in the SOL hypereutectic structure

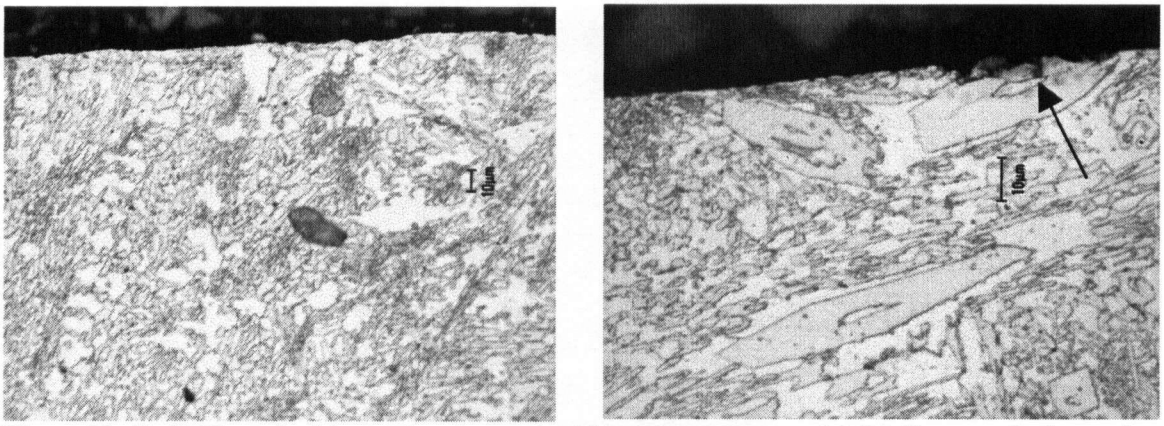

Figure 23: (Left) Finer double overlay chrome carbide microstructure. (right) Coarser single overlay chrome carbide microstructure shows signs of cracking (arrowed).

showed signs of cracking and spalling, whereas the finer dendritic structure in the DOL material showed little signs of cracking or spalling. In general, the SOL structure seems coarser and more brittle, compared to the finer DOL structure. These are atypical structures for these products. They were supposed to be hypereutectic with the DOL material containing less dilution with the base metal, resulting in an increased carbide volume fraction.

4.2.3 Tungsten Carbide Overlay Microstructures

As mentioned there were three different formulations of tungsten carbide materials tested. Two contained monolithic carbides (WC) and one had eutectic carbides (WC/W_2C). One of the monolithic carbide bearing materials was based in a soft nickel alloy matrix (WC2) and the other was based in a harder nickel alloy matrix (WC3). The harder nickel alloy matrix was used with the eutectic carbide (WC1). Figure 24 illustrates the eutectic and monolithic carbides. The best performing tungsten carbide material, as shown in Figure 20, was the eutectic carbide (WC1). Figure 24 shows little cracking of the eutectic primary carbides (arrowed in the micrograph on the left hand side). However the monolithic carbides, also shown in Figure 24, show signs of micro-cracking and micro-spalling.

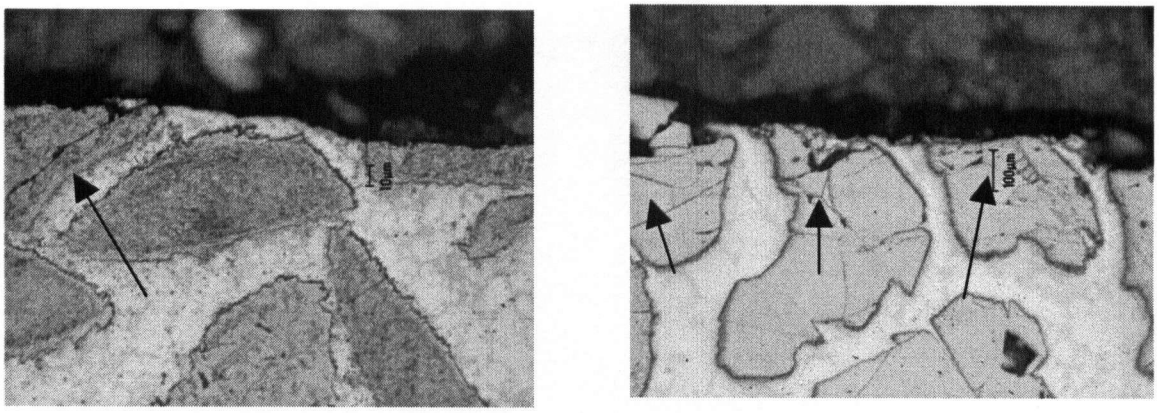

Figure 24: (Left) WC1 tungsten carbide overlay material with eutectic carbides, showing rare carbide cracking. (Right) WC 3 tungsten carbide overlay material with monolithic carbide showing extensive carbide cracking.

4.3 Selected Wear Surface Comparisons

The gouging abrasion test has been described as a closed three body abrasion test (Tylczak, 2004). For this type of test, the wear scars are expected to be a combination of rolling and sliding wear. This leads to the possibility of scarring from micro-fracture and micro-fatigue as well as straight plowing, grooving or cutting. The observed wear scars were similar for most materials, typically distinguished by the depth of the scar. The surface hardness played a roll in controlling the depth of the scar.

The samples viewed under scanning electron microscope conditions were taken from the area of the wear plate that had the highest amount of wear. This area was typically 5 mm up from the bottom of the plate. In addition, the micrographs are typical scarring patterns of the samples viewed, unless otherwise indicated.

4.3.1 Rolled Steel Wear Surface Comparison

Figure 25 compares the wear scars on the Q&T 100 plate (240 HB) and the AR 600 plate (552 HB). The Q&T 100 plate is the reference and softest material used in the gouging abrasion test. The AR 600 steel is the hardest rolled steel tested. The wearing patterns are similar. Both show deep aligned micro-scratching indicative of micro-plowing/grooving. The AR 600 plate showed more retained crushed rock compared to the reference plate. There are also micro-scratches on top of micro-scratches for both these steels as shown buy the arrows in Figure 25.

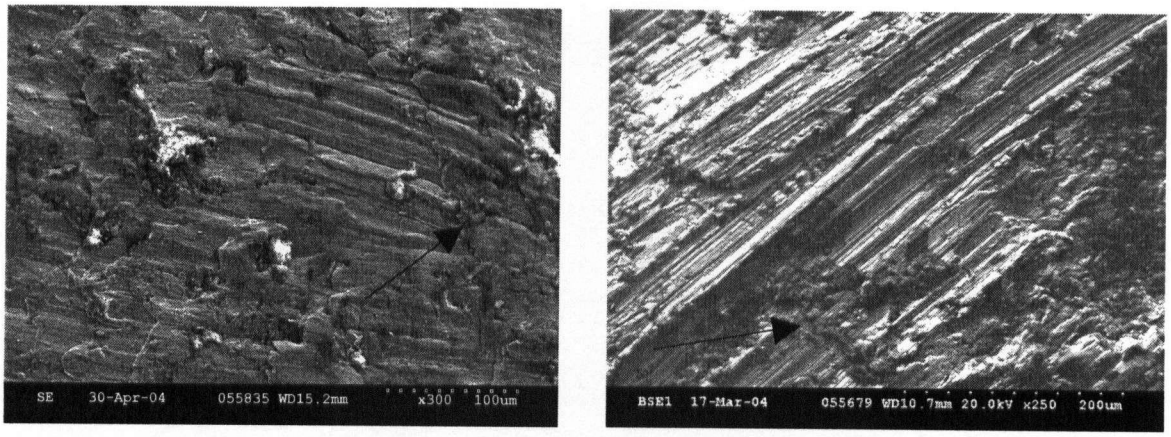

Figure 25: Aligned micro-scratching of the Q&T reference plate (right) and the AR 600 steel plate (left).

4.3.2 White Iron and Tungsten Carbide Wear Surface Comparison

Both materials show similar aligned micro-scratching seen in the rolled steels (Figure 25). However, the rolled steels showed a larger area of increased attack, making it difficult to distinguish between micro-scratches, whereas both the WC and CrMo white iron materials from Figure 26 have smaller areas of increased attack which show individual micro-scratches. A comparison of hardness between the mineralogy of the abrasive and the wear material shows that most of the constituents of the abrasive have a lower surface hardness than the WC primary carbides (Figure 11), but a higher surface hardness compared to the measured rolled steel values. The result is less surface damage to the WC test plate during testing compared to the rolled steels. The white iron is the hardest material tested (755 HB) however there is evidence of indentation to the right of the wear scars, as indicated with arrows. From the microstructure evaluation (Figure 21), the indentations are characteristic of the deformed eutectic microstructure.

The WC material displayed deeper grooves, with higher ridges. The ridges on either side of the groove are characteristic of micro-ploughing as compared to micro-scratching. This material contained the monolithic carbide which displayed the largest

amount of cracking and spalling. The darker areas (example circled in Figure 26) are inferred to be cracked or worn carbides.

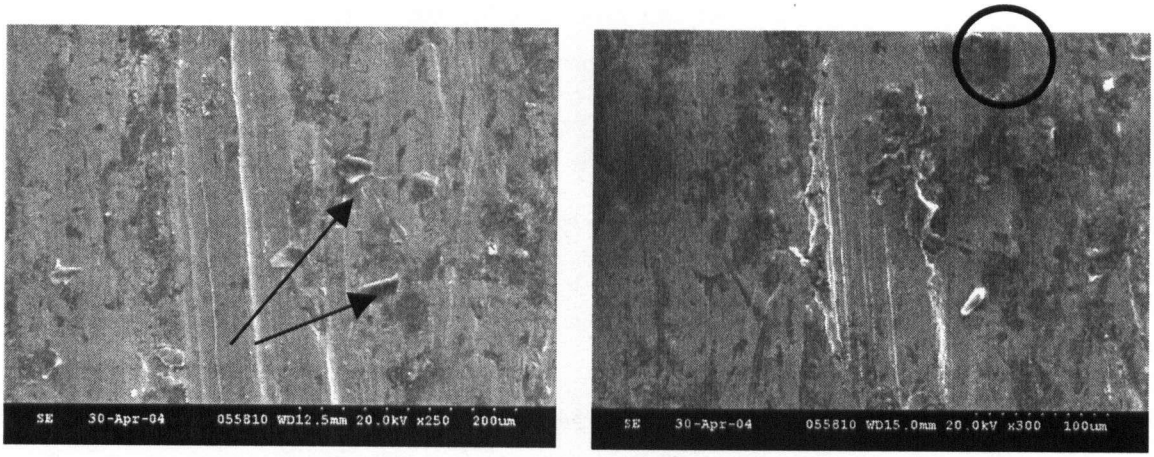

Figure 26: Surface wear scars on the CrMo white iron (left) and the WC3 PTAW tungsten carbide overlay (right).

Although the measured tungsten carbide overlay surface hardness values were much lower than the white iron surface hardness values, their surface scars appear to be similar. Figure 26 compares the wear scars seen on the laminated CrMo white iron and the tungsten carbide wear plate with the monolithic carbide and hard nickel alloy binder. The reported surface hardness values of the WC materials are lower than expected (500 HB), but they were the hardest to cut with the 10" abrasive saw used to section tested wear plates indicating their microstructure may have been much harder than what was measured.

4.3.3 Double and Single Overlay Chrome Carbide Wear Surface Comparison

The double and single overlay chrome carbide overlay materials provide a good opportunity to compare surface scars of a hypereutectic structure with a hypoeutectic dendritic structure. The surface scars of these two materials are presented in Figure 27. The hypereutectic single overlay material shows shallow, aligned micro-scratching,

whereas the hypoeutectic double overlay structure shows severe non-aligned micro-scratching. Both micrographs show little retained abrasive. The DOL wear surface examined in Figure 27 is not typical of the rest attack area, however it does qualitatively show the amount of damage/stress imposed on the plate during testing. Even though its surface looks more damaged than the SOL material, the DOL test plate had the second lowest wear factor and performed better than the SOL test plate.

The single overlay wear plate shows the dark patches (circled in Figure 27) inferred to be cracked and spalling primary carbides similar to those seen on the tungsten carbide overlay. The hypoeutectic structure displayed by the double overlay material does not show the same kind of dark patches suggesting a tougher microstructure.

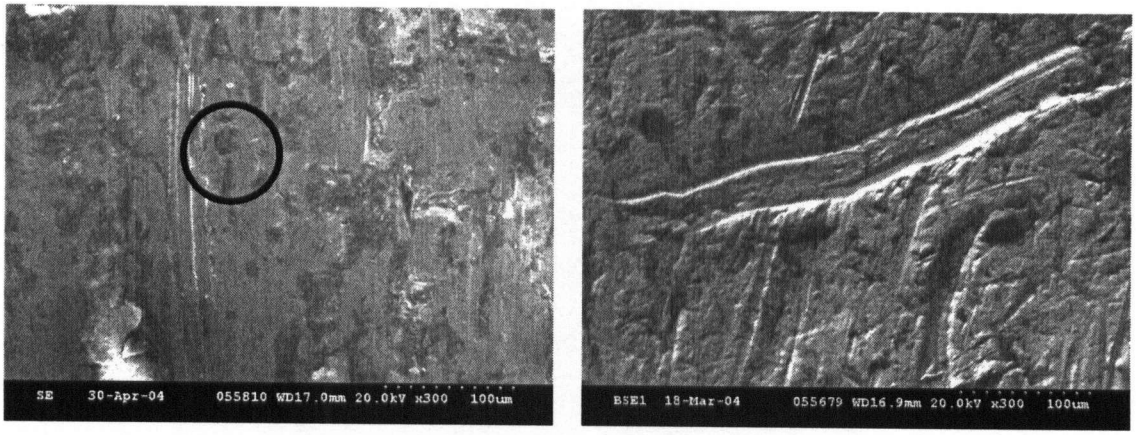

Figure 27: Wear surface of the DOL Chrome Carbide (right) and SOL chrome carbide (left)

4.4 Wear Rate

The gouging abrasion test simulates wear encountered in an actual jaw crusher very accurately. Having tested fifteen different wear materials with a limited variety of abrasives and different amounts of material comminuted, there is an opportunity to attempt to estimate wear life of the wear plates in a jaw crusher.

Estimating the wear rate of the different wear materials was completed in three different forms. The categories are; test plate wear rate, reference plate wear rate and total wear rate, all reported in cubic millimeters per kilogram (mm^3/kg). The different categories provided the opportunity to check the consistency of the jaw crusher test. The reference steel wear rate shows relative consistency throughout all trials, regardless of the amount of abrasive tested.

The wear rate is a different parameter than the wear factor. The wear factor uses the reference steel to normalize each test, whereas the wear rates are calculated independent of the reference steel and they are based on the volume loss of the test material. Figure 28 is a plot of the total wear rates as a combination of the reference material wear rates and the test material wear rates. As is shown, the reference steel wear rate makes up the bulk of the total wear rate, making the total wear rate for completely

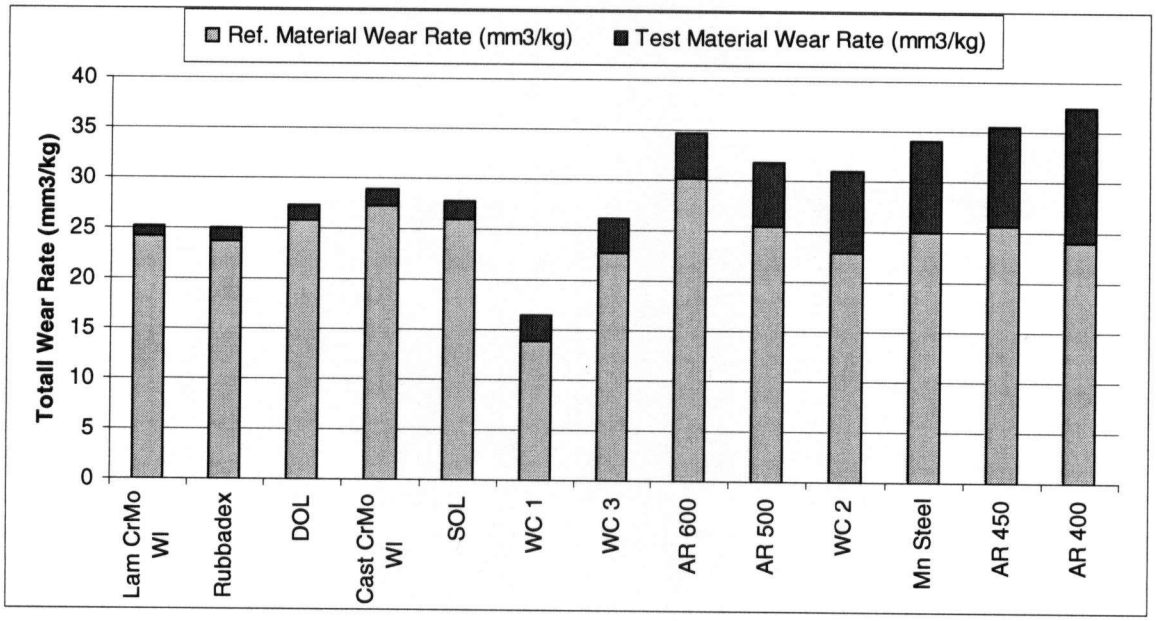

Figure 28: Contributions to the total wear rate by the reference material (stripped) and test material (solid).

different materials relatively similar. This also supports the use of reference material to normalize the gouging abrasion test. By separating the wear rates of the reference and test material it is possible to then view the impact of the reference material on the wear factor. However, it first must be shown that the reference material was wearing at the same rate for all tests. Figure 29 shows the wear rates of the reference materials. Of note are the wear rates of the tungsten carbide (WC1) and the AR600 materials. The WC1 material's wear rate is much lower than the rest. This may adversely affect the material's ranking in the gouging abrasion resistance test. It may in fact be lower than indicated (i.e. it has a higher wear factor). On the other hand, the reference material wear rate for the AR600 test is much higher that the other materials tested. As a result the AR600 test may actually have a smaller wear factor than originally calculated (i.e. a better gouging abrasion resistance). Overall there is good agreement among the reference material wear rates; those who do not agree do not influence the best performing materials. The

hypereutectic material, both cast and laminated, were not included in the wear rate calculations because of the spalling from the edges of the test plates.

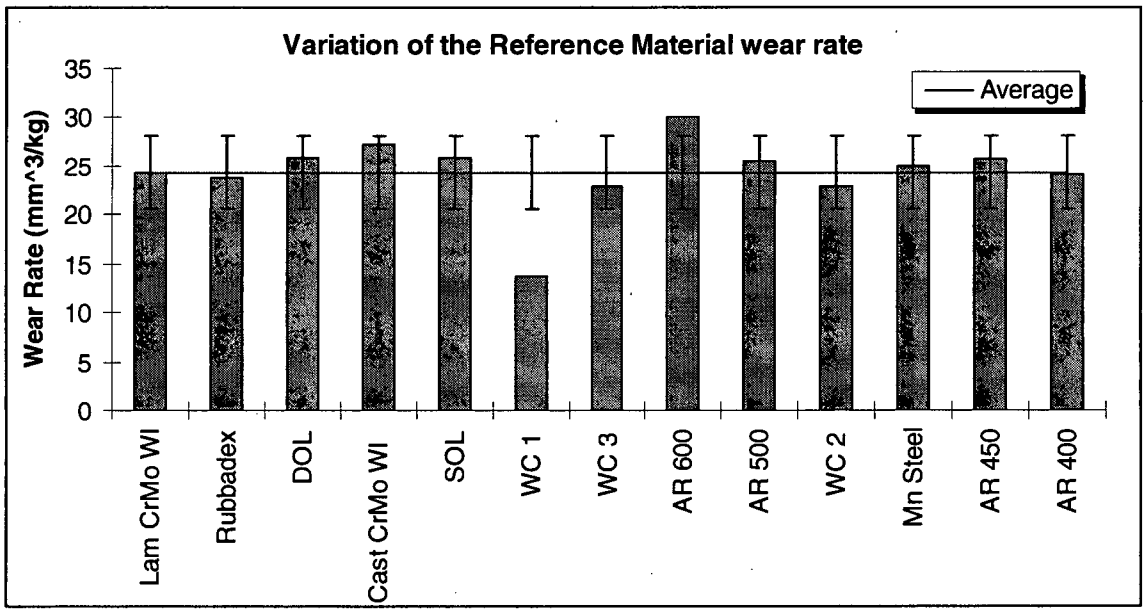

Figure 29: The variation in the reference material wear rate including the average reference material wear rate, average and standard deviation.

4.5 Influence of Abrasive on Wear Factor and Wear Rate

4.5.1 Wear Factor

Different abrasives were used to measure the affect of the abrasive on the wear factor. Figure 30 shows a linear relationship between quartz content and the wear factor. This graph suggests that as the quartz content increases, the wear factor also increases. The test plates for this series of tests were all the same, the AR 500 quench and tempered steel. The Valley and Lornex material were tested twice, the aggregate sample was tested once.

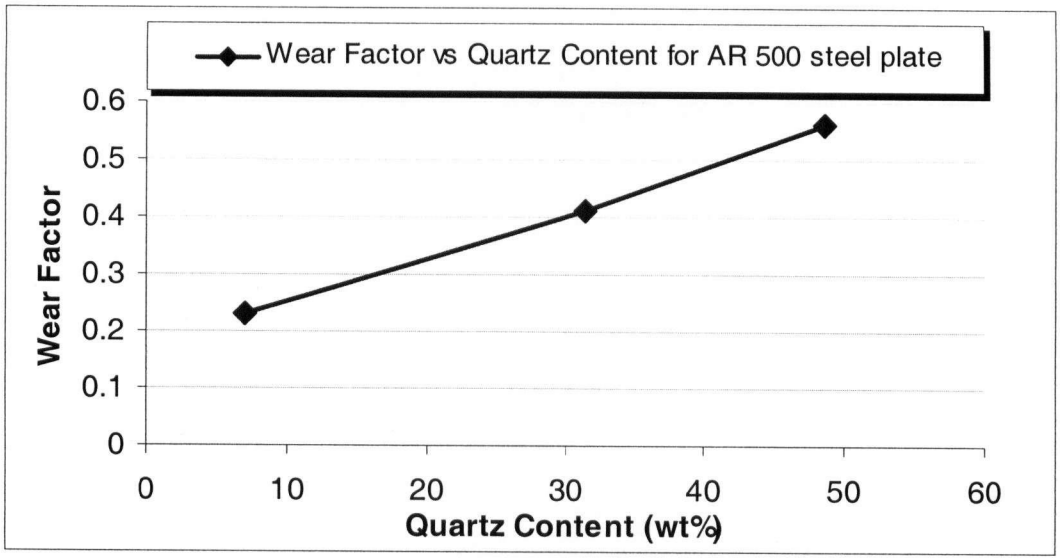

Figure 30: A linear relationship between quartz content and the wear factor for the AR 500 quenched and tempered steel plate.

4.5.2 Wear Rate

For the most part, the reference steel has the same wear rate for the same abrasive (the largest variation is in the Valley crush, whose wear rates vary between 6 mm^3/kg and 9 mm^3/kg). Figure 31 shows the contribution of the reference and test materials to the total wear rates for different abrasives.

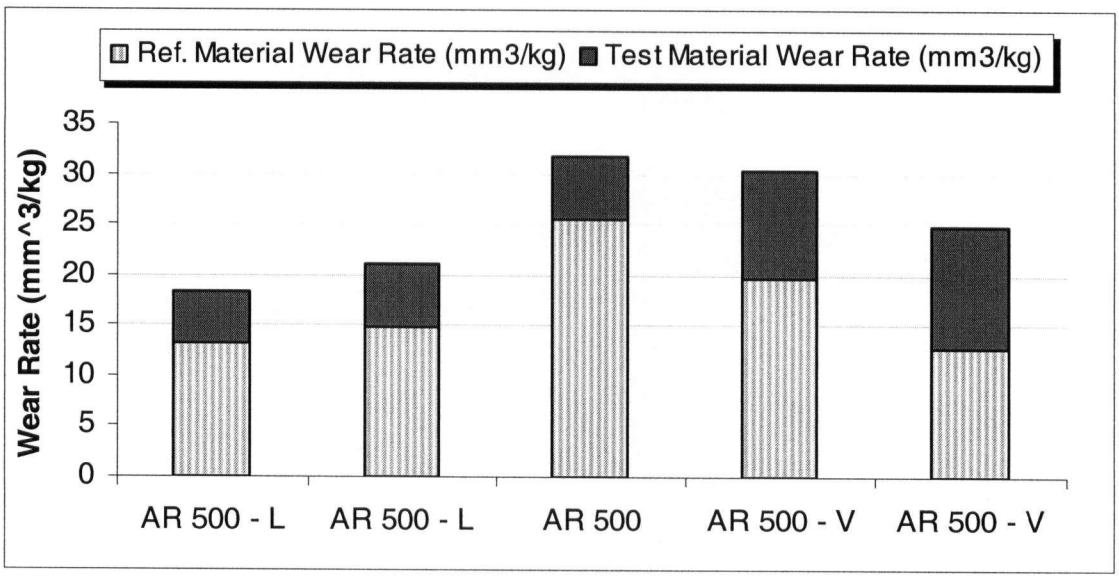

Figure 31: Contribution of reference material and test material to the total wear rate for different abrasives. L is the Lornex abrasive, V is the Valley abrasive and the middle test is the ASTM recommended abrasive (aggregate).

5.0 Summary and Discussion

5.1 Wear Factor

5.1.1 Manganese Steel

The austenitic manganese steel had a disappointing wear factor performance. It showed work hardening on both the crushing and non crushing side. The crushing side work hardened up to 450 HB, which explains the similar wear factor to the AR 450 test plate. The non-crushing side was not as hardened as the crushing side, only measuring 375 HB. Both sides did not work harden to the full potential of this product (~550 HB) (Llewellyn, 1996). The manganese steel was tested in the first phase of testing which included only 450 kg of abrasive. Because the manganese steel had not fully work hardened, it can be assumed that had it been tested with the full 907 kg of abrasive, its wear factor would have been smaller.

5.1.2 White Iron and DOL Chrome Carbide Wear Factor Comparison

The first group in Figure 20 (the wear factor comparison) contains the CrMo white irons (Rubbadex and the laminated and unlaminated versions) plus the DOL chrome carbide. Their wear factors are all below 0.06. Figure 32 shows a comparison between all the tests performed on the above mention materials. The laminated, cast and DOL materials were tested twice. The Rubbadex material was tested once. The laminated CrMo white iron consistently had the lowest wear factor. However, its eutectic microstructure showed more evidence of deformation and indentation (Figure 21) than the hypoeutectic microstructure of the DOL chrome carbide (Figure 23). All the tests on the other materials from group one had similar wear factors.

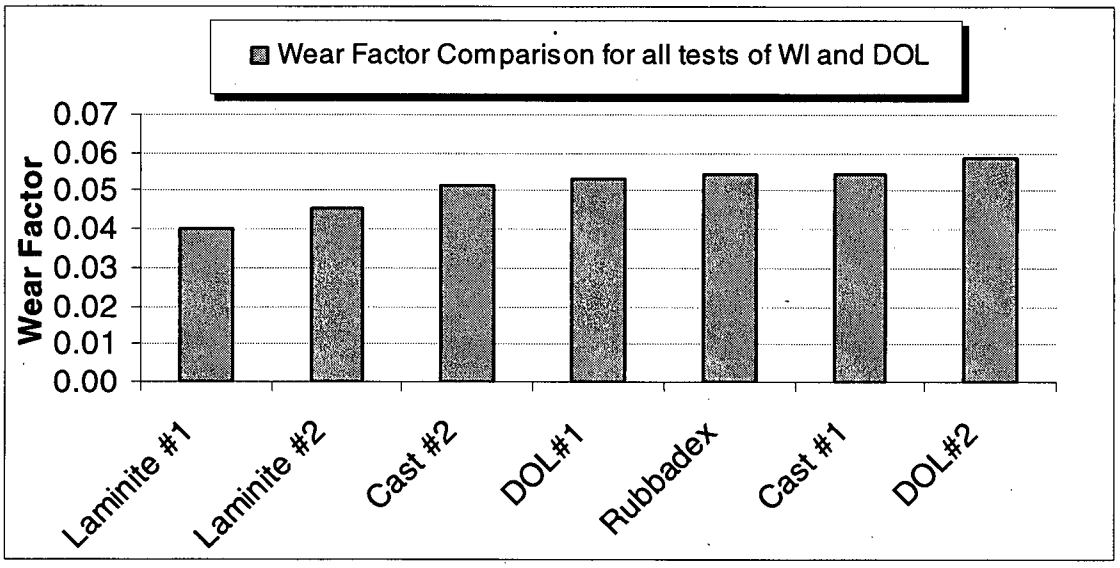

Figure 32: Wear Factor comparison of all test completed on CrMo white iron or double overlay chrome carbide material. Note: the number next to the test material name indicates the test number.

Figure 32 suggests that the laminated version of the CrMo white iron is more suitable to gouging abrasion resistant than either the cast version or the much softer DOL chrome carbide. It also suggests that the gouging abrasion resistance of the hypoeutectic DOL overlay is equivalent to the gouging abrasion resistance of the cast white iron.

5.1.3 Summary

The poor performance of the tungsten carbide material in the gouging abrasion test is believed to be due to the brittleness of hard carbides. The primary carbides contained in the tungsten carbide material could not withstand the high contact forces faced during crushing as evidenced in Figure 24 where the carbides are cracking and spalling.

Comparing all the microstructures, it seems that a fine microstructure has better gouging abrasion resistance than a coarse microstructure. A good example is the comparison of the hypoeutectic/eutectic double overlay (DOL) chrome carbide with the

eutectic/hypereutectic single overlay (SOL) chrome carbide. The SOL material showed a coarse microstructure containing a few primary carbides that were cracked. The DOL material showed a finer dendritic structure that shows no signs of cracking or spalling. Also the eutectic chromium-molybdenum white iron compared to the hypereutectic chromium white iron showed the same result. The larger primary carbides of the hypereutectic structure cracked and were flaking out, whereas the smaller eutectic carbides of the CrMo white iron showed deformation and no cracking.

It was observed in section 5.1.2 that the laminated version of the CrMo white iron consistently had the lowest wear factor and the highest gouging abrasion resistance. White irons are typically very hard, but are brittle and crack easily. By laminating the brittle white iron to a steel backing plate, the overall wear plate is less brittle and can withstand more impact/indentation type abrasion without cracking. It is inferred that the lamination helped reduce the minimal wear caused by indentation abrasion resulting in the slightly lower wear factor in comparison with the rest of group one.

5.2 Wear Rates

5.2.1 Test Materials Wear Rates

It has been shown that there is relative consistency in the wear rate of the reference material it is therefore possible to discuss the test material wear rate independently. Should the prediction be deemed accurate, it would enable the operator to gauge a time during which they should start evaluating the wear of the jaws of a crusher in service.

The wear rates are compared against each other in Figure 33. The laminated CrMo white iron had the lowest wear factor and the lowest wear rate. The wear rates were plotted against the quartz content of the various abrasives in Figure 34 and it shows an interesting result. Granted there are only three points, but it appears that there is an optimum quartz content at which the wear rate is the lower. The Lornex abrasive sample contained 31.6 wt% quartz while the aggregate sample contained only 7.1 wt% quartz. With the Lornex sample having a slightly lower wear rate.

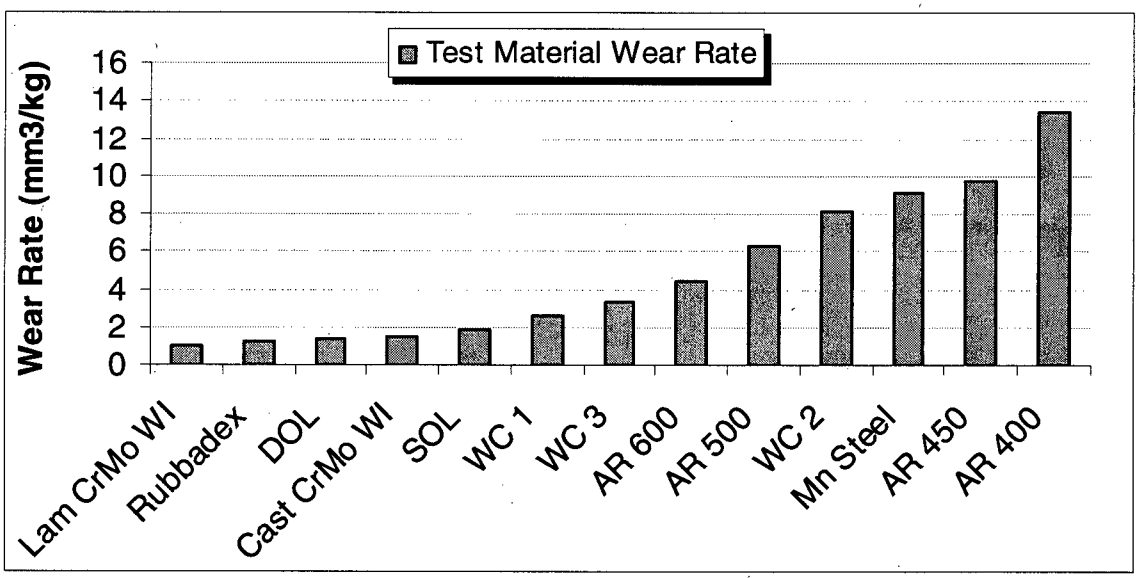

Figure 33: Wear Rates for test materials.

This is also contrary to what is shown in Figure 30 (wear factor vs quartz content plot). The wear factor is calculated according to mass loss, the wear rates are based on the same mass loss. The conflicting results may reside in the weight loss per jaw. The characteristic dip of Figure 34 is also shown in Figure 35, a comparison of mass lost during the test per jaw for the different abrasives.

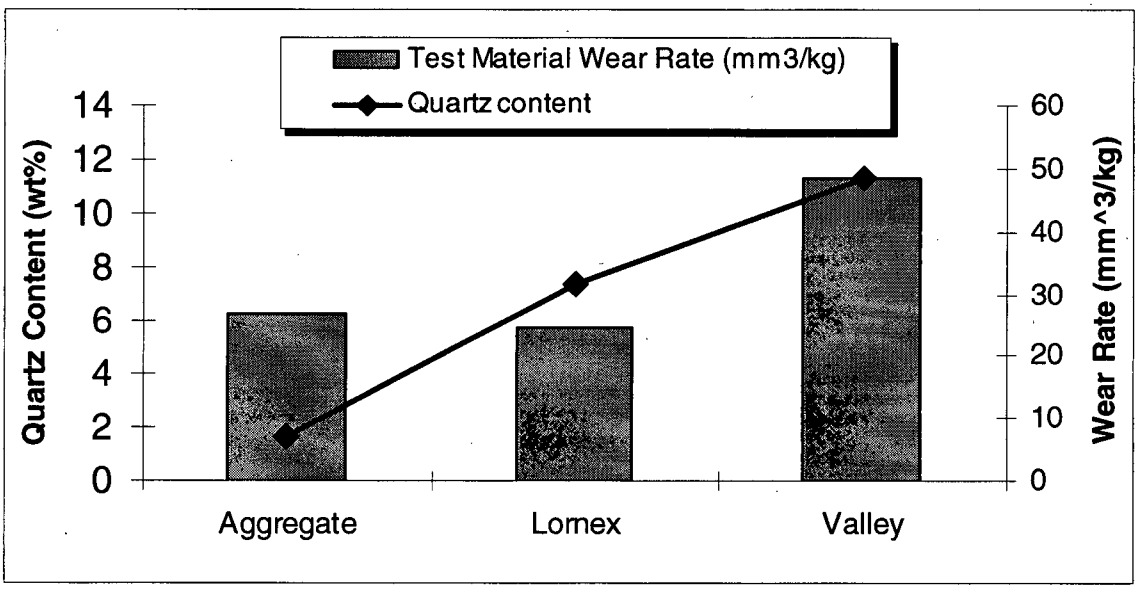

Figure 34: The quartz content of different abrasives and the associated wear rate from the same test material (AR 500).

The amount of mass lost per test is dependant on the crusher jaw. It is evident after testing that the stationary jaw suffers more gouging abrasion than does the moveable jaw. Figure 35 also indicates that the amount of attack not only varies per jaw, but varies per jaw per quartz content. It seems that the moveable test jaw has a linear relationship between mass lost and quartz content, while the stationary jaw has a non-linear relationship between mass lost and quartz content. The same non-linear relationship that is evident when correlating the wear rate with quartz content in Figure 34. Figure 30 is normalized by using the reference steel and a combination of both jaws therefore it does not show the non-linear weight loss that is seen to occur in Figure 35. As these plots are in the beginning stages of development. To make better correlations, further testing should be done with a greater variety of abrasives.

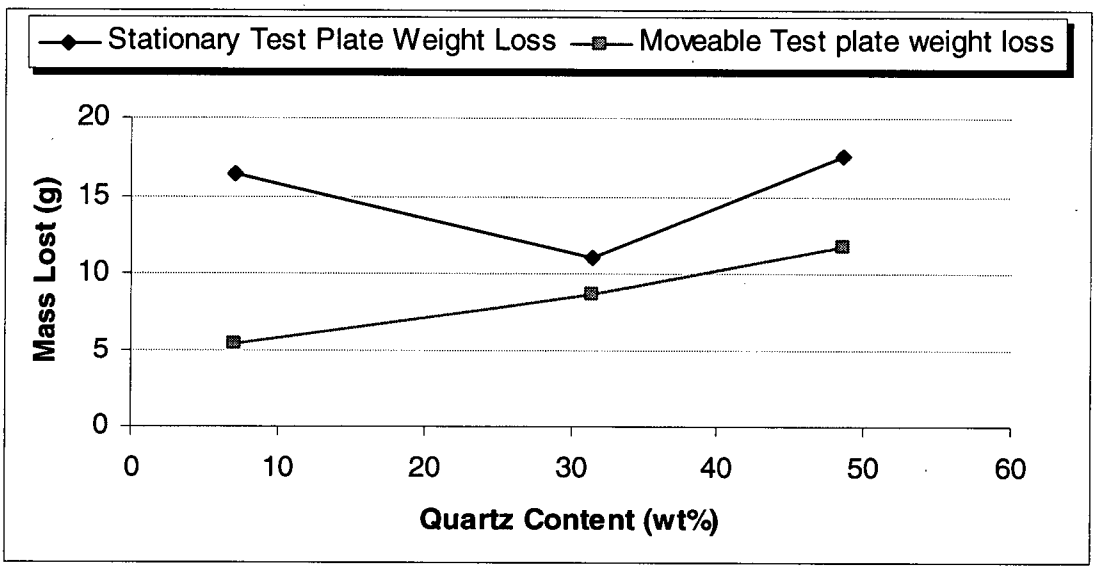

Figure 35: Plot of the mass lost per jaw during testing vs the quartz content of the abrasive.

5.2.2 Summary

The wear rate is used in an attempt to estimate how long a wear plate will last in service. These are laboratory test results that have not been correlated to field data. However the values are logical. The ranking of wear factors and wear rates is presented in Table 7 and discrepancies explained in section 5.3. The wear rates are reported as mm^3/kg. When comparing these results it is important to remember that a cubic millimeter is not very much and these wear rates are for gouging abrasion conditions only. Also, differences between laboratory and field crushing conditions will most probably exist. The most fundamental difference will be the abrasive. The abrasive used during testing was chosen and uniform. It is unlikely that a crusher will encounter a uniform abrasive throughout its service life. However it is believed that this is a strong step forward in attempting to predict the life of wear liners.

5.3 Wear Factor vs Wear Rate

Table 7 contains the two different rankings of the test material. The first column ranks the materials according to their wear factor (normalized) and the second column ranks the materials according to their wear rate (not normalized). The tungsten carbide materials have a different ranking as a result of A) the different wear rates of the reference material in the WC 1 test and B) the different densities of the carbide vs the matrix. Factor B has noticeably decreased the tungsten carbide wearing rate relative to rolled steels and the other members of the third group from Figure 20. Again the materials from group one of Figure 20, the DOL chrome carbide and the CrMo white iron (rubbadex and cast versions) have very similar rankings. The laminated CrMo has the lowest wear rate and wear factor.

Test Material Wear Factor	Test Material Wear Rate
Lam CrMo WI	Lam CrMo WI
Cast CrMo WI	Rubbadex
Rubbadex	DOL
DOL	Cast CrMo WI
SOL	SOL
AR 600	WC 1
WC 1	WC 3
AR 500	AR 600
WC 3	AR 500
Mn Steel	WC 2
AR 450	Mn Steel
AR 400	AR 450
WC 2	AR 400

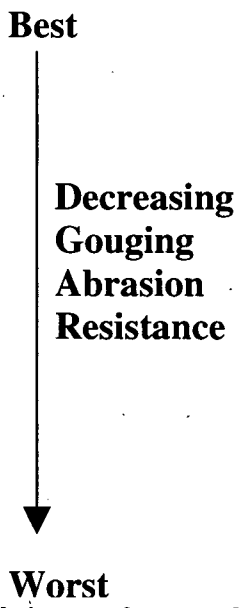

Table 7: A comparison of the rankings of the test materials according to their wear factor and their wear rate.

5.4 Influence of Surface Hardness on the Wear Factor

In an effort to predict the gouging abrasion resistance of a material the surface hardness was graphed against the wear factor. Surface hardness has been shown to ably predict the performance of materials in high stress and low stress abrasion tests (Hawk, 1999),(Tylczak, 1999). However, gouging abrasion resistance does not share the same relationship. It has been shown that the results of low stress and high stress abrasion tests performed at the Albany Research Center in the United States provide a linear relationship between surface hardness and wear factor, leading to the general statement that a harder material has a higher resistance to high or low stress abrasive wear. It should be noted that the testing program at the Albany Research Center consisted of steels and irons only (Tylczak, 1999). The Albany Research Center also performed a version of the gouging abrasion test. Its results are similar to the ones obtained during this program. Figure 36 shows the relationship between surface hardness and gouging abrasion resistance for this work. It does not include the austenitic manganese steel wear plate whose gouging abrasion resistance is mentioned in section 5.1.1. Gouging abrasion resistance increases (decrease in wear factor) rapidly until approximately 575 HB. After which there seems to be minor changes in gouging abrasion resistance for large changes in surface hardness.

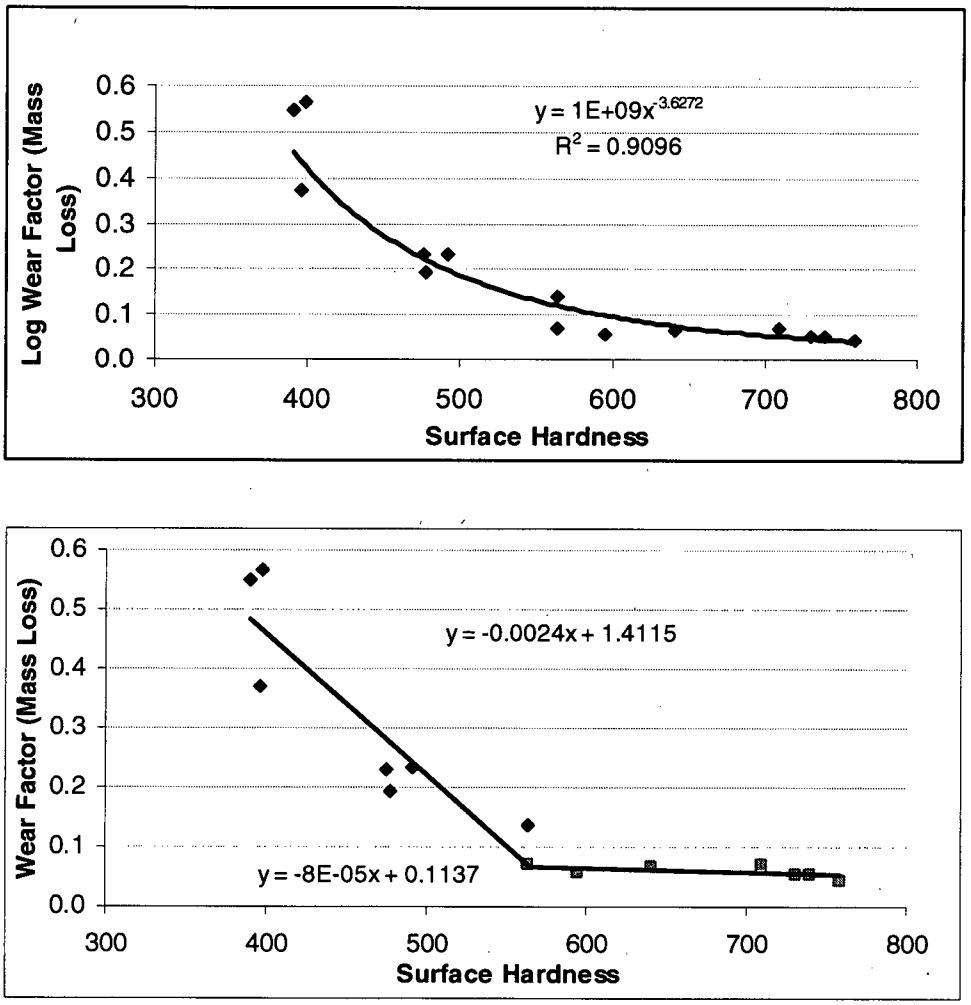

Figure 36: Wear factor vs Surface hardness of the different materials tested (bottom) two distinct trends, (top) power law fit of the data.

Figure 36 also shows a power law relationship fitting a plot of all the wear factors vs surface hardness. Ideally the surface hardness would be a good first indicator of the wear factor however there are many different types of materials tested. Each material draws its surface hardness from different parts of its microstructure. The rolled steels and austenitic manganese steel rely on the matrix, while the overlays and various white irons rely on a combination of matrix and carbide performance. Typically the carbides are much harder than the matrix giving the overlay and white iron materials higher surface

hardness values without much change in their gouging abrasion resistance. The testing has shown there is enough contact force to disturb the microstructure of the wear plate affecting entire carbides, resulting in similar wear factors for a given surface hardness above 575 HB. Therefore the surface hardness is not the best method to predict the wear factors for gouging abrasion situations.

Figure 37 shows the wear factor for the rolled steels vs their surface hardness. The rolled steels are all made in a similar manner (slightly different compositions and different quench and tempering techniques) and are rated according to their surface hardness. In addition they all have similar microstructures. Although the main focus of this testing program was the overlay materials, the trend of the rolled steels is an interesting result. It shows that for this type of wear plate, the surface hardness is in fact a good tool to estimate the wear factor.

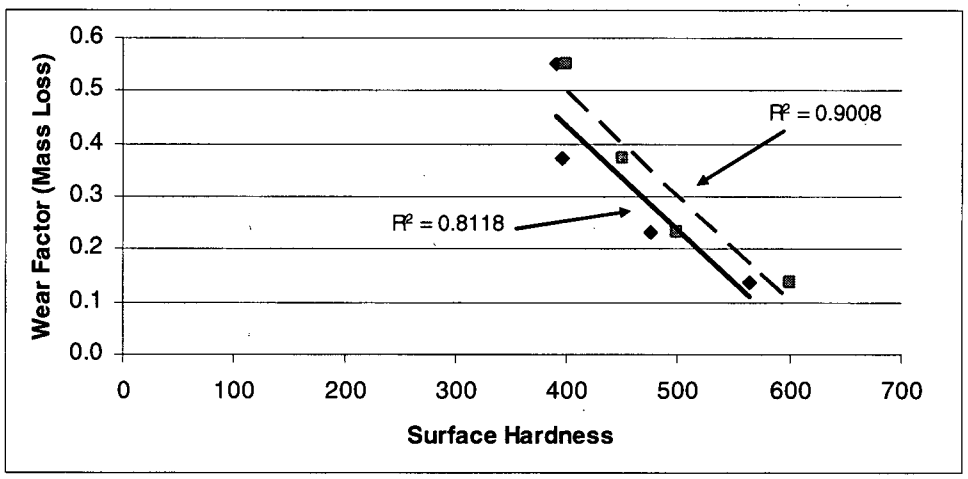

Figure 37: Wear factor vs measured surface hardness (diamonds) and rated surface hardness (square) for rolled steels.

The points plotted as squares in Figure 37 are the measured surface hardness values. The diamonds in Figure 37 are the rated surface hardness values. At the time of hardness measurement, the plates were ground to remove any decarburized layer that develops at the surface of a wear plate. The decarburized layer is not as hard as the rest of the plate, affecting the measured surface hardness values. There is no guarantee that the entire decarburized layer was removed before testing.

5.5 Summary

The tungsten carbide overlay provided quite a few interesting results in the wear factor portion of this thesis. Firstly, the measured surface hardness values were below what was expected and secondly, the poor gouging abrasion resistance (high wear factor). In addition, it was found that a finer microstructure has a higher gouging abrasion resistance compared to a coarser structure.

The results also demonstrate that the surface hardness played a large role in the creation of the surface scars. The harder the surface, the shallower the wear scars. The abrasive used for most of the testing was concrete aggregate whose major constituent is

volcanic rocks. The volcanics are slightly harder than the AR 600 steel, but not as hard as the white irons tested. As a result the materials whose surface hardness is lower than that of the AR 600 steel suffered severe attack, characterized by the wear scars observed on the Q&T 100 reference steel wear plate and the AR 600 test steel wear plate (Figure 25). Whereas the materials whose surface hardness were harder than the AR600 steel showed less attack characterized by the individual wear scars visible under the SEM on the WC overlays and laminated CrMo white iron test plates (Figure 26).

As mentioned in sections 2.2 and 4.5, the abrasive is an important factor in attempting to predict wear life. A correlation between the wear factor and the wear rates against quartz content was attempted; unfortunately only three different abrasives were available for testing. The goal was to create a plot that would link a material parameter, with an abrasive parameter and give an estimate of the wear rate. The first step taken was to have a uniform wear material, the AR 500 steel, and vary the abrasive and complete the tests. The next step would have been to observe the results and decide on a course of action. The results were unforeseen. While the quartz content provided a linear relationship when graphed against the wear factor, it gave a non-linear relationship when graphed against the wear rate. From the data produced during this thesis, it seems that there is an optimum quartz content at which the wear rate is the lowest. As previously mentioned in sections 3.3 the wear factor is calculated using the volume loss from both jaws and is normalized with the reference steel. The wear rate is calculated without the reference steel. A plot of the test material mass lost per jaw against quartz content (Figure 35) shows the non-linear relationship is as a result of the test material mass loss

on the stationary plate. There are many factors that could influence the wear rate on the stationary plate; from the wear mechanism, to the type of wear and the efficiency of the motor moving the jaws (providing a uniform stress throughout testing on the particles).

6.0 Conclusions and Future Work

6.1 Conclusions

This thesis has the shown the benefits of using laboratory gouging abrasion testing in assessing the relationship between material and abrasive properties and material wear. The work presented has been successful in developing a more detailed knowledge about the behavior of material wear in gouging abrasion situations in mining applications with immediate impacts in the oil sands industry.

This thesis provided information for the following relationships;

- There is an optimum surface hardness at which the wear factor does not change significantly with large changes in surface hardness (~575 HB).
- Taking into account the decarburized layer at the surface of some of the AR steels, there is a linear relationship between the wear factor and surface hardness
- There appears to be a linear relationship between the wear factor and quartz content of the abrasive.
- There appears to be an optimum quartz content at which the wear rate is lowest (~30 wt% qz).
    - Each jaw in the crusher suffers unique wear. The moveable jaw weight loss shows a non-linear trend against quartz content, while the stationary jaw weight loss shows a linear trend with quartz content.

On the enhancement of gouging abrasion knowledge this thesis has demonstrated the following:

- A finer microstructure is more gouging abrasion resistant than a coarser microstructure.
- The laminated CrMo white iron material has the best gouging abrasion resistance of all the materials tested.
- The double overlay chrome carbide material was among the best performers during testing. While the single overlay chrome carbide materials was not as gouging abrasion resistant. Both microstructures were atypical for this product.
- The hypereutectic white irons (both cast and laminated) are not as well suited to gouging abrasion applications.
- The primary WC carbides of the tungsten carbide overlay material are too brittle to have successful application in gouging abrasion conditions.
- The AR600 steel has the highest gouging abrasion resistance of the Abrasion Resistant steels tested. It ranks better than some of the tungsten carbide materials, but not as good as the hypereutectic white irons.

The objective of developing a document that would assist in educating the mine engineer on wear and wear materials was successfully completed in this work. However, further work has to be completed to properly relate field trials to laboratory tests. In the author's opinion, the jaw crusher presents the most realistic opportunity to relate

laboratory wear rates to observed field wear rates. In addition further testing is required on the relationships between wear rates and quartz content, which produced unusual results.

6.2 Future Work

A couple of novel ideas and surprising results have been presented in this thesis. Most require further justification. The correlation between microstructure and gouging abrasion resistance should have additional testing by performing more gouging abrasion tests and high stress and low stress abrasion tests. The gouging abrasion tests will confirm the results presented and the other abrasion tests will see if the relationship stretches into other areas of abrasion.

In addition, work should be done to relate the gouging abrasion test results to field analysis. Evaluating the wearing mechanisms of different wear materials in service and comparing them with the wearing mechanisms of the laboratory appears to be a good place to start. Historically, the wear factor or variation thereof has been used in attempting to correlate a laboratory test to a field trial. However, comparing the surface scars, metallography and wear factor is more likely to derive a proper correlation. Also, a comparison of the wear rates presented here with those observed in the field would further strengthen the relationship between laboratory tests and field trials.

The correlation between wear rates, a material property and quartz content is a potentially powerful tool. However this type of correlation will need large amounts of data to be accurate, much the same way the stability graph works for assessing the

stability of underground openings, as a result further gouging abrasion testing is required. Logically the next step would be to keep the same three abrasives and change the wear material or continue with the same test material but comminute different abrasives.

Another indicator that could possibly be used to correlate to the wear rate and a wear material property is the abrasivity index. It is a combination of the unconfined compressive strength and the quartz content. The abrasivity index is commonly used to predict drill bit life and it takes into account the mechanical properties of the rock, such as Young's modulus, Poisson's ratio and tensile strength. In the author's opinion, primary crushing comminutes rocks big enough to have their mechanical properties influence the wear rate of the crusher.

There has been no mention of power consumption during the gouging abrasion test. There is extensive data concerning the power consumption of primary crushers and mills in general that may help correlate the laboratory results to field trials. Power measurements can also provide the researchers with another correlation to estimate either the wear factor or wear rate.

Finally most materials were tested only once. Additional tests should be performed to ensure reproducibility of the results. In particular, the DOL and SOL materials, because of their atypical microstructures, should be tested again.

References

A Strategy for Tribology in Canada, (1st ed). (1986). National Research Council Canada Associate Committee on Tribology.

Alloy Steel International (2004) Retrieved February 13th, 2004 from http://www.alloysteel.net/english/4_wear_factors.asp

American Society for the Testing and Materials. (2004) Abrasive Wear. Retrieved March 25, 2004, from http://www.asminternational.org/hbk/do/highlight/content/V18/D03/A03/B0001193.html

Arnson, H.L., Parks, J.L., & Larsen, D.R., (1980) Alloys and Designs for Large Mill Liners and Crusher Parts.

Bednarz, B., (1999) Abrasive Wear of hardfacing materials, *Australasian Welding Journal, 44,* 40-43

Beste, U., Lundvall, A., Jacobson, S., (2004). Micro-scratch evaluation of rock types – a means to comprehend rock drill wear. *Tribology International, 37,* 203-210.

British Columbia Ministry of Energy and Mines (2004) Retrieved on May 20th, 2004 from http://www.nrcan.gc.ca/gsc/pacific/vancouver/earthsci/index_e.htm

Burwell, J.T., (1957). Survey of Possible Wear Mechanisms. *Wear, 1,* 119-141

Conduto, D.P., (1999) *Geotechnical Engineering: Principals and Practices.* Upper Saddle River, New Jersey, Prentice Hall.

Deniz, V., Ozdag, H., (2003) A new approach to Bond grindability and work index: dynamic elastic parameters, *Minerals Engineering, 16,* 211-217.

Donovan, J.G., (2003) Fracture toughness based models for the prediction of power consumption, product size and capacity of Jaw Crusher,

Dodd, J., (1979) Further Progress in the Development and Utilization of Abrasion Resistant Alloys in the U.S., *International Abrasion Colloquim, 4th,* 11-1 – 11-17.

Ersay, J.D., Marshall, A.W. & Proschan, F., (1973) Shock models and wear processes, *The annals of Probability, Vol 1 No. 4,* 627-649.

Gates, J.D. (1998). Two-body and three-body abrasion: A critical discussion. *Wear, 214,* 139-146.

Gore, G.J., Gates, J.D., (1997). Effect of hardness on three very different forms of wear, *Wear, 203-204,* 544-563

Hartman. (Ed.) (1992) *SME Mineral Processing Handbook*, New York: Society of Mining Engineers.

Hawk, J.A., Wilson, R.D., Tylczak, J.H. & Doğan, Ö.N., (1999). Laboratory abrasive wear tests: investigation of test methods and alloy correlation. *Wear, 225-229,* 1031-1042.

Liang, P. (2004) NRC Internal Report

Llewellyn, R.J., Dolman, K.F., (2004a). High Chromium White Irons for Slurry Pump Service in Mineral Processing, CIM 2004.

Llewellyn, R.J. (2004b) UBC Mining Lecture on Wear

Llewellyn R.J., Tolfree, D., Liang, P., Hall. R.A., (2004c), Gouging abrasion assessment of materials of the oil sands industry, CIM 2004.

Llewellyn, R.J., Leith, W., Magel, E., (Eds).(1996) Wear Materials Guider for the Mining and Mineral Processing Industry, *The Mining Association of British Columbia.*

Lindqvist M., Evertsson, C.M., (2003) Liner wear in jaw crushers, *Minerals Engineering, 16,* 1-12.

Marks, G.L., Mutton, P.J., Watson, J.D., (1976) Gouging Abrasion Tests on several Irons and Steels, *Broken Hill Proprietary Melbourne Research Laboratory Report*

Mercer, A., (1961) Some Simple Wear-Dependant Renewal Processes, *Journal of The Royal Statistics Society, Series B (Methodological),* 32, 368-376

Moore, M.A., (1974) A review of two-body abrasive wear,

Moshgbar, M., Parkin, R.M. and Bearman, R.A., (1994) *The Compensation of Liner Wear for Optimum control of Cone Crushers*, Progress in Mineral Processing Technology, 549-555.

Park, K.S., (1988a) Optimal Continous – Wear Limit Replacement under Periodic Inspections. *IEEE Transactions on Reliability, 37,* 97-102

Park, K.S., (1988b) Optimal Continous – Wear Limit Replacement with Wear-Dependant failures. *IEEE Transactions on Reliability, 37,* 293-294

Peterson, M.B., Winer, W.O., (Eds)(1980) Wear Control Handbook, *American Society of Mechanical Engineers.*

Qian, M.A., Chaochang, W., (1997) Impact-abrasion behaviour of low alloy white cast irons, *Wear, 209*, 308-315.

Rabinowicz, E., Dunn, L.A., Russell, P.G., (1961) A study of abrasive wear under three-body conditions. *Wear, 4,* 345-355.

Rabinowicz, E, (1995) *Friction and Wear of Materials,* Wiley, New York

Radziszewski, P., (1997) Predictive Model for Ball Mill Wear, *Canadian Metallurgical Quarterly,* 36, 87-93

Sare, I.R., Constantine, A.G., (1997) Development methodologies for the evaluation of wear resistant materials for the mineral industry, *Wear, 203-204*, 671-678.

Stachowiak, G.B., Stachowiak, G.W., (2001). The effects of particle characteristics on three-body abrasive wear. *Wear, 249,* 201-207

Stachowiak, G.B., Stachowiak, G.W., (2004). Wear mechanisms in ball-cratering tests with large abrasive particles, *Wear, 256,* 600-607

Tang, C.A., Xu, X.H., Kou, S.Q., Lindqvist, P.-A., Liu, H.Y., (2001) Numerical investigation of particle breakage as applied to mechanical crushing – Part I: Single-particle breakage, *International Journal of Rock Mechanics & Mining Sciences, 38,* 1147-1162.

Tang, C.A., Xu, X.H., Kou, S.Q., Lindqvist, P.-A., Liu, H.Y., (2001) Numerical investigation of particle breakage as applied to mechanical crushing – Part II: Inter-particle breakage, *International Journal of Rock Mechanics & Mining Sciences, 38,* 1163-1172.

The British Gear Association (2004) Retrieve May 20th, 2004 from http://www.bga.org.uk/publish/techpub/tn/TRTN1_4.htm

Trezona, R.I., Allsopp, D.N. & Hutchings, I.M., (1999). Transitions between two-body and three-body abrasive wear: influence of test conditions in the microscale abrasive wear test. *Wear, 225-229,* 205-214.

Tylczak, J.H., Hawk, J.A., Wilson, R.D., (1999) A comparison of laboratory abrasion and field wear results. *Wear, 225-229,* 1059-1069.

Utley, R., (2002) Selection and Sizing of Primary Crushers, in Mular A., Halbe D., Barrat D., (Eds.), Mineral Processing Plant Design, Practice and Control proceedings (pg 584-605).

Vingsbo, O., (1979) Wear and Wear Mechanims, *International Conference on Wear of Materials,* American Society of Mechanical Engineers, 620-635

Watson, J.D., Mutton, P.J., Sare, I.R., (1980) Abrasive Wear of White Cast Irons, *Metals Forum, Vol 3 No. 1,* 75-88

Wirojanupatump, S., Shipway, P.H., (1999) A direct comparison of wet and dry abrasion behaviour of mild steel, *Wear, 233-235,* 655-665.

APPENDIX 1

Laboratory Data for Quartz Content Calculations

Quantitative Phase Analysis of Samples "Valley." And "Lornex" Using the Rietveld Method and X-ray Powder Diffraction Data.

Attention:
Donald Tolfree
Mining Engineering Dept. UBC

Mati Raudsepp, Ph.D.
Elisabetta Pani, Ph.D.

Dept. of Earth & Ocean Sciences
6339 Stores Road
The University of British Columbia
Vancouver, BC V6T 1Z4

May 12, 2004

EXPERIMENTAL METHOD

The particle size of the samples "Valley" and "Lornex" was further reduced to the optimum grain-size range for X-ray analysis (<5 μm) by grinding under ethanol in a vibratory McCrone Micronising Mill (McCrone Scientific Ltd., London, UK) for 7 minutes. Fine grain-size is an important factor in reducing micro-absorption contrast between phases.

Step-scan X-ray powder-diffraction data were collected over a range 3-70°2θ with CuKα radiation on a standard Siemens (Bruker) D5000 Bragg-Brentano diffractometer equipped with a diffracted-beam graphite monochromator crystal, 2 mm (1°) divergence and antiscatter slits, 0.6 mm receiving slit and incident-beam Soller slit. The long fine-focus Cu X-ray tube was operated at 40 kV and 40 mA, using a take-off angle of 6°.

RESULTS AND DISCUSSION

The X-ray diffractograms were analyzed using the International Centre for Diffraction Database PDF-4 using Search-Match software by Siemens (Bruker). X-ray powder-diffraction data were refined with Rietveld Topas 2.1 (Bruker AXS). The Rietveld refinement plots are given in Figures 1-2. The results of quantitative phase analysis by Rietveld refinement are given in Table 1.

Table 1: Results of quantitative analysis from Rietveld refinements (wt.%)

Phase	Ideal Formula	Valley	Lornex
Quartz	SiO_2	48.6	31.5
K-Feldspar	$KAlSi_3O_8$	7.0	7.0
Plagioclase	$NaAlSi_3O_8 - CaAl_2Si_2O_8$	29.1	40.0
Muscovite	$KAl_2AlSi_3O_{10}(OH)_2$	11.4	14.2
Biotite	$K(Mg,Fe^{2+})_3AlSi_3O_{10}(OH)_2$		1.0
Chlorite	$(Mg,Fe^{2+})_5Al(Si_3Al)O_{10}(OH)_8$		1.6
Kaolinite	$Al_2Si_2O_5(OH)_4$	1.3	0.8
Gypsum	$CaSO_4 \cdot 2H_2O$	1.1	
Ankerite	$Ca(Fe^{2+},Mg,Mn)(CO_3)_2$		0.5
Calcite	$CaCO_3$	1.1	2.5
Pyrite	FeS_2		0.4
Magnetite	$Fe^{2+}Fe_2^{3+}O_4$	0.4	0.5
Total		100.0	100.0

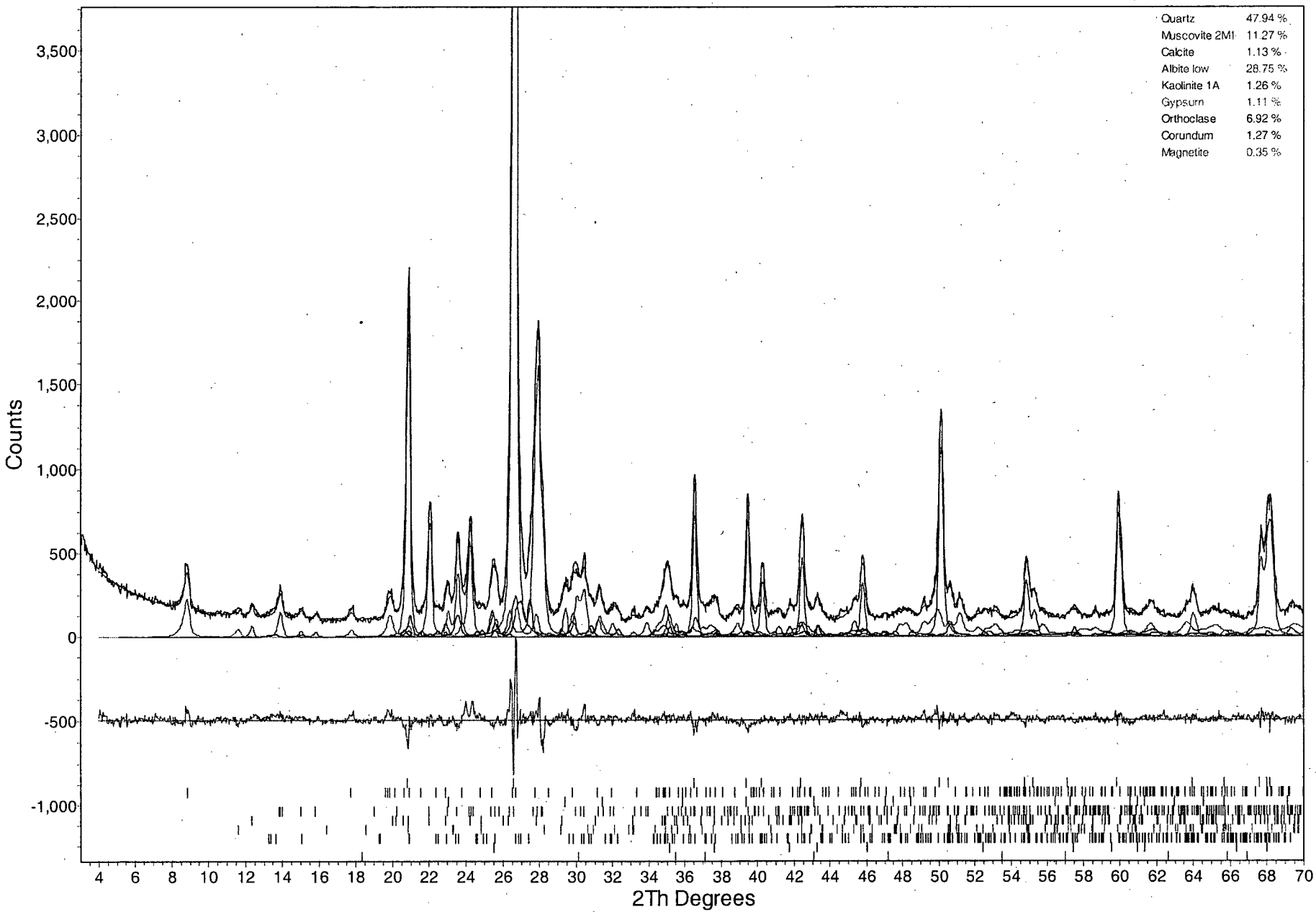
Quartz 47.94 %
Muscovite 2M1 11.27 %
Calcite 1.13 %
Albite low 28.75 %
Kaolinite 1A 1.26 %
Gypsum 1.11 %
Orthoclase 6.92 %
Corundum 1.27 %
Magnetite 0.35 %
Counts
3,500
3,000
2,500
2,000
1,500
1,000
500
0
-500
-1,000
4 6 8 10 12 14 16 18 20 22 24 26 28 30 32 34 36 38 40 42 44 46 48 50 52 54 56 58 60 62 64 66 68 70
2Th Degrees

Figure 1: . Rietveld refinement plot for sample **Valley** (blue line - observed intensity at each step; red line - calculated pattern, solid grey line below – difference between observed and calculated intensities; vertical bars, positions of all Bragg reflections. Coloured lines are individual diffraction patterns of all phases

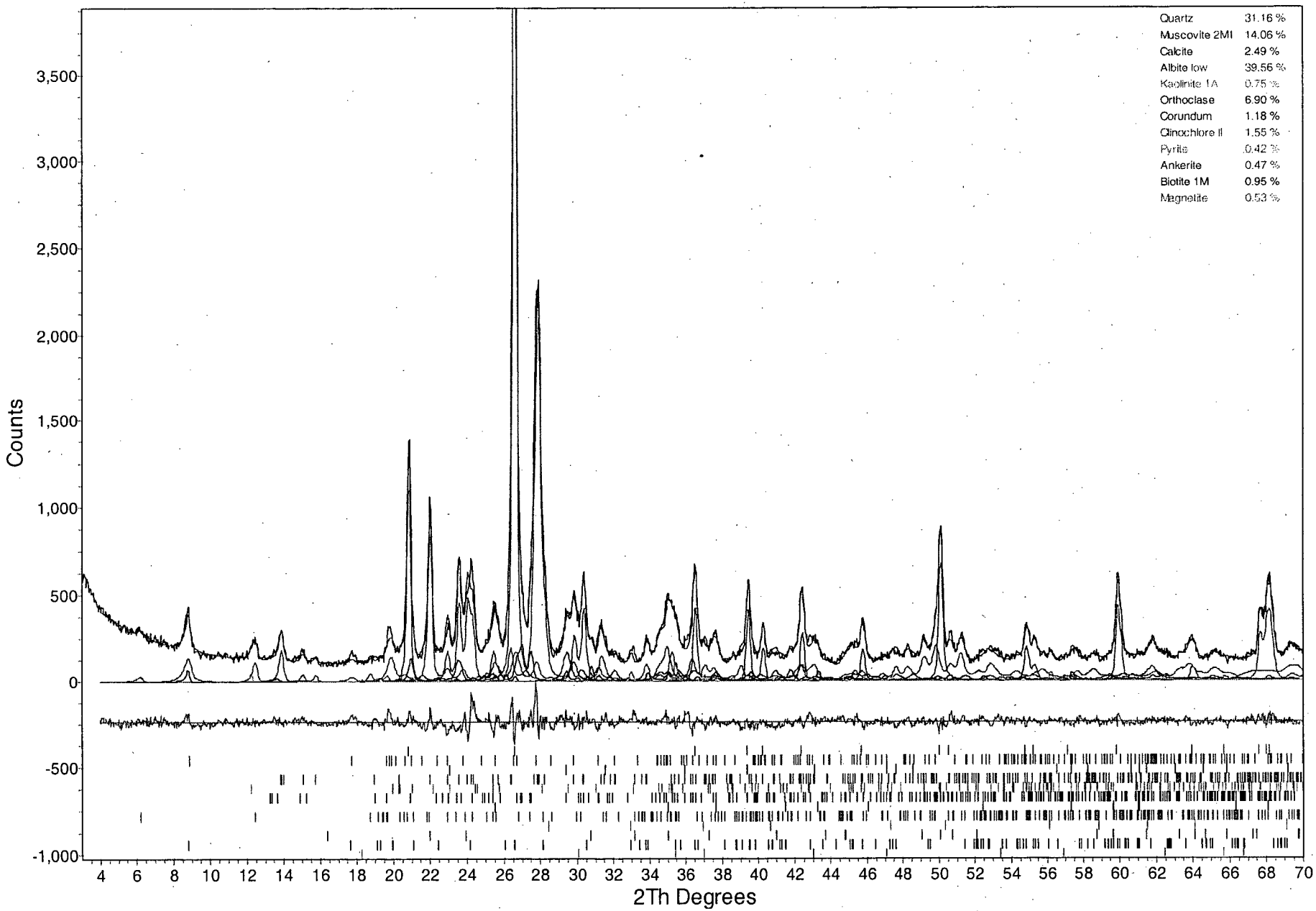
Quartz 31.16 %
Muscovite 2M1 14.06 %
Calcite 2.49 %
Albite low 39.56 %
Kaolinite 1A 0.75 %
Orthoclase 6.90 %
Corundum 1.18 %
Clinochlore II 1.55 %
Pyrite 0.42 %
Ankerite 0.47 %
Biotite 1M 0.95 %
Magnetite 0.53 %
Counts
3,500
3,000
2,500
2,000
1,500
1,000
500
0
-500
-1,000
4 6 8 10 12 14 16 18 20 22 24 26 28 30 32 34 36 38 40 42 44 46 48 50 52 54 56 58 60 62 64 66 68 70
2Th Degrees

Figure 2: . Rietveld refinement plot for sample **Lornex** (blue line - observed intensity at each step; red line - calculated pattern, solid grey line below – difference between observed and calculated intensities; vertical bars, positions of all Bragg reflections. Coloured lines are individual diffraction patterns of all phases

APPENDIX 2

Detailed Wear Factor Calculations

Manganese Steel

Plate	OQE-4	OQE-3	OPY-2A	OPY-1A
Position	SR	ML	SL	MR
Weight Before (g)	2109.7	2155.2	2456.5	2447.6
Weight After (g)	2090.2	2141.6	2396.0	2417.3
Difference (g)	19.5	13.6	60.5	30.3
Tonnage Crushed (kg)	454	Aggregate		
Wear Factor	**0.386**			

Manganese Steel

Plate	OQE-1	OQE-2	OPY-1	OPY-2
Position	SR	ML	SL	MR
Weight Before (g)	2130.4	2172.2	2266.2	2258.0
Weight After (g)	2108.9	2164.2	2214.9	2228.3
Difference (g)	21.5	8.0	51.3	29.7
Tonnage Crushed (kg)	454	Aggregate		
Wear Factor	**0.344**			

Cast CrMo White Iron

Plate	OQM-1	OQM-2	OPY-6	OPY-8
Position	SR	ML	SL	MR
Weight Before (g)	2348.7	2349.0	2418.3	2430.3
Weight After (g)	2344.5	2347.7	2353.4	2395.8
Difference (g)	4.2	1.3	64.9	34.5
Tonnage Crushed (kg)	454	Aggregate		
Wear Factor	**0.051**			

AR 400 Steel

Plate	OQA-1	OQA-2	OPY-3A	OPY-5A
Position	SR	ML	SL	MR
Weight Before (g)	2454.7	2444.7	2454.2	2472.8
Weight After (g)	2424.4	2428.8	2402.2	2441.9
Difference (g)	30.3	15.9	52.0	30.9
Tonnage Crushed (kg)	454	Aggregate		
Wear Factor	**0.549**			

AR 500 Steel

Plate	OQC-1	OQC-2	OPY-4	OPY-5
Position	SR	ML	SL	MR
Weight Before (g)	2441.8	2466.5	2435.5	2422.4
Weight After (g)	2425.4	2461.2	2381.1	2389.0
Difference (g)	16.4	5.3	54.4	33.4
Tonnage Crushed (kg)	454	Aggregate		
Wear Factor	**0.230**			

AR 450 Steel

Plate	OQB-2	OQB-1	OPY-3	OPY-9
Position	SR	ML	SL	MR
Weight Before (g)	2449.3	2528.8	2417.5	2411.0
Weight After (g)	2425.6	2517.5	2359.3	2377.2
Difference (g)	23.7	11.3	58.2	33.8
Tonnage Crushed (kg)	454	Aggregate		
Wear Factor	**0.371**			

AR 600 Steel

Plate	OQD-2	OQD-1	OPY-6A	OPY-8A
Position	SR	ML	SL	MR
Weight Before (g)	2441.1	2431.6	2455.6	2433.9
Weight After (g)	2429.3	2427.9	2389.5	2396.1
Difference (g)	11.8	3.7	66.1	37.8
Tonnage Crushed (kg)	454	Aggregate		
Wear Factor	**0.138**			

Rubbadex

Plate	OQO-1	OQO-3	OQR-11	OQR-3
Position	SR	ML	SL	MR
Weight Before (g)	2751.1	2774.5	3179.2	3171.9
Weight After (g)	2748.8	2772.4	3135.0	3134.1
Difference (g)	2.3	2.1	44.2	37.8
Tonnage Crushed (kg)	454	Aggregate		
Wear Factor	**0.054**			

Laminated CrMo White Iron

Plate	OQN-1	OQN-3	OQR-5	OQR-4
Position	SR	ML	SL	MR
Weight Before (g)	2859.9	2894.5	2946.7	2929.8
Weight After (g)	2857.8	2892.5	2903.0	2883.2
Difference (g)	2.1	2.0	43.7	46.6
Tonnage Crushed (kg)	454	Aggregate		
Wear Factor	**0.045**			

Cast CrMo White Iron

Plate	OQM-3	OQM-4	OPY-10	OPY-7A
Position	SR	ML	SL	MR
Weight Before (g)	2395.5	2337.5	2423.7	2458.6
Weight After (g)	2389.0	2334.1	2320.3	2383.9
Difference (g)	6.5	3.4	103.4	74.7
Tonnage Crushed (kg)	454	Aggregate		
Wear Factor	**0.054**			

Laminated CrMo White Iron

Plate	OQN-2	OQN-4	OQR-8	OQR-9
Position	SR	ML	SL	MR
Weight Before (g)	2955.7	2960.5	3062.1	3043.5
Weight After (g)	2954.8	2960.0	3035.5	3025.1
Difference (g)	0.9	0.5	26.6	18.4
Tonnage Crushed (kg)	454	Aggregate		
Wear Factor	**0.031**			

Laminated CrMo White Iron

Plate	OQN-2	OQN-4	OQR-8	OQR-9
Position	SR	ML	SL	MR
Weight Before (g)	2955.7	2960.5	3062.1	3043.5
Weight After (g)	2953.8	2959.2	3014.8	3006.7
Difference (g)	1.9	1.3	47.3	36.8
Tonnage Crushed (kg)	454	Aggregate		
Wear Factor	**0.038**			

Laminated CrMo White Iron

Plate	OQN-2	OQN-4	OQR-8	OQR-9
Position	SR	ML	SL	MR
Weight Before (g)	2955.7	2960.5	3062.1	3043.5
Weight After (g)	2952.8	2958.7	2995.9	2992.4
Difference (g)	2.9	1.8	66.2	51.1
Tonnage Crushed (kg)	454	Aggregate		
Wear Factor	**0.040**			

Laminated CrMo White Iron

Plate	OQN-2	OQN-4	OQR-8	OQR-9
Position	SR	ML	SL	MR
Weight Before (g)	2955.7	2960.5	3062.1	3043.5
Weight After (g)	2951.8	2958.3	2977.9	2978.0
Difference (g)	3.9	2.2	84.2	65.5
Tonnage Crushed (kg)	454	Aggregate		
Wear Factor	**0.040**			

Double Overlay Chrome Carbide

Plate	OQR-21	OXO-10	OXO-3	OQR-23
Position	ML	MR	SL	SR
Weight Before (g)	2481.1	2497.6	2486.6	2497.2
Weight After (g)	2383.2	2493	2482.2	2422
Difference (g)	97.9	4.6	4.4	75.2
Tonnage Crushed (kg)	908	Aggregate		
Wear Factor	**0.053**			

Double Overlay Chrome Carbide

Plate	OQR-26	OXO-8	OXO-7	OQR-18
Position	ML	MR	SL	SR
Weight Before (g)	2461.5	2467.8	2472.1	2453.1
Weight After (g)	2356.6	2462.4	2467	2374.9
Difference (g)	104.9	5.4	5.1	78.2
Tonnage Crushed (kg)	908	Aggregate		
Wear Factor	**0.058**			

Single Overlay Chrome Carbide

Plate	OXN-6	OQR-1	OQR-2	OXN-8
Position	ML	MR	SL	SR
Weight Before (g)	2496.6	2481.2	2470.5	2428.7
Weight After (g)	2486.8	2369	2389.9	2425.3
Difference (g)	9.8	112.2	80.6	3.4
Tonnage Crushed (kg)	908	Aggregate		
Wear Factor	**0.065**			

Single Overlay Chrome Carbide

Plate	OXN-4	OQR-36	OQR-37	OXN-2
Position	MR	ML	SR	SL
Weight Before (g)	2456.5	2500.3	2565	2526.3
Weight After (g)	2451.4	2429.4	2471.4	2518.6
Difference (g)	5.1	70.9	93.6	7.7
Tonnage Crushed (kg)	908	Aggregate		
Wear Factor	**0.077**			

Weight Loss Wear Factor

Tungsten Carbide 1 (WC1)

Plate	OVO-1	3	OVO-2	35
Position	MR	ML	SL	SR
Weight Before (g)	2605.5	2459.7	2495.1	2488
Weight After (g)	2590.4	2391.6	2482.1	2409.1
Difference (g)	15.1	68.1	13	78.9
Tonnage Crushed (kg)	908	Aggregate		
Wear Factor	**0.193**			

Tungsten Carbide 3 (WC3)

Plate	OVP-1	34	OVP-2	13
Position	ML	MR	SR	SL
Weight Before (g)	2567.5	2466.5	2470.8	2434.7
Weight After (g)	2546.3	2387.6	2455.2	2356.3
Difference (g)	21.2	78.9	15.6	78.4
Tonnage Crushed (kg)	908	Aggregate		
Wear Factor	**0.234**			

Tungsten Carbide 2 (WC2)

Plate	OVQ-1	5	OVQ-2	12
Position	SR	SL	ML	MR
Weight Before (g)	2544.2	2501.9	2520.4	2503.9
Weight After (g)	2492.5	2411.3	2482.4	2485.2
Difference (g)	51.7	90.6	38	67.4
Tonnage Crushed (kg)	908	Aggregate		
Wear Factor	**0.567**			

Density of Materials		
OVO (WC1)	0.01173	g/mm^3
OVQ (WC2),OVP (WC3)	0.01217	g/mm^3
Reference Steel	0.0076	g/mm^3

Volume Loss Wear Factor

Tungsten Carbide 1 (WC1)

Plate	OVO-1	3	OVO-2	35
Position	MR	ML	SL	SR
Volume Before (mm^3)	222122.8	323644.7	212711	327368.4
Volume After (mm^3)	220835.5	314684.2	211602.7	316986.8
Difference (mm^3)	1287.298	8960.526	1108.269	10381.58
Tonnage Crushed (kg)	908	Aggregate		
Wear Factor	**0.125**			

Tungsten Carbide 3 (WC3)

Plate	OVP-1	34	OVP-2	13
Position	ML	MR	SR	SL
Volume Before (mm^3)	210969.6	324539.5	203023.8	320355.3
Volume After (mm^3)	209227.6	314157.9	201742	310039.5
Difference (mm^3)	1741.988	10381.58	1281.841	10315.79
Tonnage Crushed (kg)	908	Aggregate		
Wear Factor	**0.146**			

Tungsten Carbide 2 (WC2)

Plate	OVQ-1	5	OVQ-2	12
Position	SR	SL	ML	MR
Volume Before (mm^3)	209055.1	329197.4	207099.4	329460.5
Volume After (mm^3)	204806.9	317276.3	203977	327000
Difference (mm^3)	4248.151	11921.05	3122.432	2509.226
Tonnage Crushed (kg)	908	Aggregate		
Wear Factor	**0.800**			

APPENDIX 3

Detailed Wear Rate Calculations

Wear Rates for 908 kg of abrasive crushed

VALLEY CRUSH

AR500	Weight Loss (g)	Volume Loss (mm^3)	Wear Rate (g/kg)	Wear Rate (mm^3/kg)
Reference Plate	43.80	5763.16	0.10	12.69
Test Plate	41.40	5447.37	0.09	12.00
Total	85.20	11210.53	0.19	24.69

AR500	Weight Loss (g)	Volume Loss (mm^3)	Wear Rate (g/kg)	Wear Rate (mm^3/kg)
Reference Plate	68.00	8947.37	0.15	19.71
Test Plate	36.50	4802.63	0.08	10.58
Total	104.50	13750.00	0.23	30.29

LORNEX CRUSH

AR500	Weight Loss (g)	Volume Loss (mm^3)	Wear Rate (g/kg)	Wear Rate (mm^3/kg)
Reference Plate	45.20	5947.37	0.10	13.10
Test Plate	17.90	2355.26	0.04	5.19
Total	63.10	8302.63	0.14	18.29

AR500	Weight Loss (g)	Volume Loss (mm^3)	Wear Rate (g/kg)	Wear Rate (mm^3/kg)
Reference Plate	51.20	6736.84	0.11	14.84
Test Plate	21.50	2828.95	0.05	6.23
Total	72.70	9565.79	0.16	21.07

AGGREGATE

Wear Rates for 908 kg of abrasive crushed

WC1	Weight Loss (g)	Volume Loss (mm^3)	Wear Rate (g/kg)	Wear Rate (mm^3/kg)
Reference Plate	147.00	12531.97	0.16	13.80
Test Plate	28.10	2395.57	0.03	2.64
Total	175.10	14927.54	0.19	16.44

WC2	Weight Loss (g)	Volume Loss (mm^3)	Wear Rate (g/kg)	Wear Rate (mm^3/kg)
Reference Plate	158.00	20789.47	0.17	22.90
Test Plate	89.70	7370.58	0.10	8.12
Total	247.70	28160.06	0.27	31.01

WC3	Weight Loss (g)	Volume Loss (mm^3)	Wear Rate (g/kg)	Wear Rate (mm^3/kg)
Reference Plate	157.30	20697.37	0.17	22.79
Test Plate	36.80	3023.83	0.04	3.33
Total	194.10	23721.20	0.21	26.12

DOL	Weight Loss (g)	Volume Loss (mm^3)	Wear Rate (g/kg)	Wear Rate (mm^3/kg)
Reference Plate	173.10	22776.32	0.19	25.08
Test Plate	9.00	1184.21	0.01	1.30
Total	182.10	23960.53	0.20	26.39

DOL	Weight Loss (g)	Volume Loss (mm^3)	Wear Rate (g/kg)	Wear Rate (mm^3/kg)
Reference Plate	183.10	24092.11	0.20	26.53
Test Plate	10.50	1381.58	0.01	1.52
Total	193.60	25473.68	0.21	28.05

SOL	Weight Loss (g)	Volume Loss (mm^3)	Wear Rate (g/kg)	Wear Rate (mm^3/kg)
Reference Plate	192.90	25381.58	0.21	27.95
Test Plate	13.20	1736.84	0.01	1.91
Total	206.10	27118.42	0.23	29.87

SOL	Weight Loss (g)	Volume Loss (mm^3)	Wear Rate (g/kg)	Wear Rate (mm^3/kg)
Reference Plate	164.50	21644.74	0.18	23.84
Test Plate	12.80	1684.21	0.01	1.85
Total	177.30	23328.95	0.20	25.69

Wear Rates for 454 kg of abrasive crushed

Manganese Steel	Weight Loss (g)	Volume Loss (mm^3)	Wear Rate (g/kg)	Wear Rate (mm3/kg)
Reference Plate	90.8	11947.37	0.20	26.32
Test Plate	33.1	4355.26	0.07	9.59
Total	123.9	16302.63	0.27	35.91

Manganese Steel	Weight Loss (g)	Volume Loss (mm^3)	Wear Rate (g/kg)	Wear Rate (mm3/kg)
Reference Plate	81.2	10684.21	0.18	23.53
Test Plate	29.5	3881.58	0.06	8.55
Total	110.7	14565.79	0.24	32.08

Cast CrMo White Iron	Weight Loss (g)	Volume Loss (mm^3)	Wear Rate (g/kg)	Wear Rate (mm3/kg)
Reference Plate	99.4	13078.95	0.22	28.81
Test Plate	5.5	723.68	0.01	1.59
Total	104.9	13802.63	0.23	30.40

AR 400 Steel	Weight Loss (g)	Volume Loss (mm^3)	Wear Rate (g/kg)	Wear Rate (mm3/kg)
Reference Plate	82.9	10907.89	0.18	24.03
Test Plate	46.2	6078.95	0.10	13.39
Total	129.1	16986.84	0.28	37.42

AR 500 Steel	Weight Loss (g)	Volume Loss (mm^3)	Wear Rate (g/kg)	Wear Rate (mm3/kg)
Reference Plate	87.8	11552.63	0.19	25.45
Test Plate	21.7	2855.26	0.05	6.29
Total	109.5	14407.89	0.24	31.74

AR 450 Steel	Weight Loss (g)	Volume Loss (mm^3)	Wear Rate (g/kg)	Wear Rate (mm3/kg)
Reference Plate	92	12105.26	0.19	25.65
Test Plate	35	4605.26	0.07	9.76
Total	127	16710.53	0.27	35.40

AR 600 Steel	Weight Loss (g)	Volume Loss (mm^3)	Wear Rate (g/kg)	Wear Rate (mm3/kg)
Reference Plate	103.9	13671.05	0.23	30.11
Test Plate	15.5	2039.47	0.03	4.49
Total	119.4	15710.53	0.26	34.60

Rubbadex	Weight Loss (g)	Volume Loss (mm^3)	Wear Rate (g/kg)	Wear Rate (mm3/kg)
Reference Plate	82	10789.47	0.18	23.77
Test Plate	4.4	578.95	0.01	1.28
Total	86.4	11368.42	0.19	25.04

Laminated CrMo White Iron	Weight Loss (g)	Volume Loss (mm^3)	Wear Rate (g/kg)	Wear Rate (mm3/kg)
Reference Plate	90.3	11881.58	0.20	26.17
Test Plate	4.1	539.47	0.01	1.19
Total	94.4	12421.05	0.21	27.36

Cast CrMo White Iron	Weight Loss (g)	Volume Loss (mm^3)	Wear Rate (g/kg)	Wear Rate (mm3/kg)
Reference Plate	178.1	23434.21	0.20	25.81
Test Plate	9.9	1302.63	0.01	1.43
Total	188	24736.84	0.21	27.24

Laminated CrMo White Iron	Weight Loss (g)	Volume Loss (mm^3)	Wear Rate (g/kg)	Wear Rate (mm3/kg)
Reference Plate	45	5921.05	0.20	26.08
Test Plate	1.4	184.21	0.01	0.81
Total	46.4	6105.26	0.20	26.90

Laminated CrMo White Iron	Weight Loss (g)	Volume Loss (mm^3)	Wear Rate (g/kg)	Wear Rate (mm3/kg)
Reference Plate	84.1	11065.79	0.19	24.37
Test Plate	3.2	421.05	0.01	0.93
Total	87.3	11486.84	0.19	25.30